Published for SISSA by Springer

Received: *May 24, 2019*
Accepted: *August 15, 2019*
Published: *September 2, 2019*

Production of muons from heavy-flavour hadron decays in pp collisions at $\sqrt{s} = 5.02$ TeV

The ALICE collaboration

E-mail: ALICE-publications@cern.ch

Abstract: Production cross sections of muons from semi-leptonic decays of charm and beauty hadrons were measured at forward rapidity ($2.5 < y < 4$) in proton-proton (pp) collisions at a centre-of-mass energy $\sqrt{s} = 5.02$ TeV with the ALICE detector at the CERN LHC. The results were obtained in an extended transverse momentum interval, $2 < p_{\mathrm{T}} < 20$ GeV/c, and with an improved precision compared to previous measurements performed in the same rapidity interval at centre-of-mass energies $\sqrt{s} = 2.76$ and 7 TeV. The p_{T}- and y-differential production cross sections as well as the p_{T}-differential production cross section ratios between different centre-of-mass energies and different rapidity intervals are described, within experimental and theoretical uncertainties, by predictions based on perturbative QCD.

Keywords: Heavy Ion Experiments

ArXiv ePrint: 1905.07207

https://doi.org/10.1007/JHEP09(2019)008

JHEP09(2019)008

Contents

JHEP09(2019)008

1 Introduction

The measurement of heavy-flavour (charm and beauty) production cross sections in proton-proton (pp) collisions at the CERN LHC represents an important test of perturbative Quantum Chromodynamics (pQCD). Due to their large masses, heavy quarks are produced almost exclusively in initial hard partonic scatterings and consequently their production cross sections can be estimated in the framework of pQCD. The calculations are based on a factorisation approach and computed as a convolution of the hard parton scattering cross section, evaluated as a perturbative series of the coupling constant of the strong interaction, the parton distribution function (PDF) of the colliding protons and the fragmentation function of heavy quarks to heavy-flavour hadrons. Heavy-flavour production cross sections are predicted at next-to-leading order (NLO) using the fixed-order plus next-to-leading logarithms (FONLL) approach [1, 2] or the general-mass variable-flavour-number scheme (GM-VFNS) [3, 4]. Calculations at leading order based on k_{T} factorisation [5] also exist. The forward rapidity range accessible by ALICE ($2.5 < y < 4$) allows us to test pQCD predictions in a region of small Bjorken x down to about 10^{-5} (x being the longitudinal momentum fraction of initial-state partons, primarily gluons). In this region, the gluon distribution functions are affected by large uncertainties [6]. The systematic uncertainties on the theoretical production cross sections are larger than the experimental ones and are dominated by the uncertainties on renormalisation and factorisation scales. Recent theoretical developments have shown that the ratios of the open heavy-flavour production cross sections between different beam energies and different rapidity intervals are promising observables which are expected to be sensitive to the gluon PDFs [6], since the uncertainties on scales become negligible with respect to the PDF uncertainties when calculating such

ratios. The production cross sections of charm, beauty and heavy-flavour hadron decay leptons measured over a wide energy domain at the Tevatron, RHIC and LHC (see e.g. [7] and references therein and, [8–16]) are described, within uncertainties, by these pQCD-based calculations at both forward and central rapidities in a large transverse momentum ($p_{\rm T}$) range. Also the ratios of D-meson production cross sections between different rapidity intervals and centre-of-mass energies recently measured by the ALICE and LHCb experiments [13, 15, 16] are described by pQCD-based predictions within uncertainties.

Furthermore, the measurement of heavy-flavour production cross sections in pp collisions provides the necessary baseline for the corresponding measurements in proton-nucleus and nucleus-nucleus collisions. These measurements allow us to study cold nuclear matter effects and effects related to the hot strongly-interacting medium, respectively.

This letter describes the $p_{\rm T}$- and y-differential measurements of the production cross sections of muons from the decay of charm and beauty hadrons in pp collisions at $\sqrt{s} = 5.02$ TeV, with the ALICE detector at the LHC. These measurements are performed at forward rapidity, in the interval $2.5 < y < 4$. They are facilitated by an experimentally triggerable observable and relatively large decay branching ratios (about 10%), thus resulting in relatively large statistics allowing for differential measurements over a wide $p_{\rm T}$ interval. The present measurements cover the interval $2 < p_{\rm T} < 20$ GeV/c, where the beauty contribution is expected to dominate over the charm contribution in the high $p_{\rm T}$ region i.e. for $p_{\rm T} > 5$ GeV/c [2]. They are complementary to those performed at the same centre-of-mass energy by the LHCb Collaboration for D-meson species in a kinematic region limited to hadron $p_{\rm T} < 10$ GeV/c [16]. Moreover, the present results are obtained in a significantly extended $p_{\rm T}$ region and the total uncertainties are reduced by a factor larger than two, compared to previous published ALICE results for muons from heavy-flavour hadron decays [17, 18].

The letter is structured as follows. Section 2 describes the apparatus with an emphasis on the detectors used in the analysis and the data taking conditions. Section 3 addresses the analysis details. Section 4 presents the results, namely the $p_{\rm T}$- and y-differential cross sections of muons from heavy-flavour hadron decays as well as the ratio of the $p_{\rm T}$-differential cross section between different centre-of-mass energies and rapidity intervals and their comparison with pQCD-based FONLL calculations. Finally, conclusions are drawn in section 5.

2 Experimental apparatus and data taking conditions

The ALICE detector and its performance are described in detail in [19, 20]. This analysis is based on muons reconstructed in the muon spectrometer which covers the pseudo-rapidity interval $-4 < \eta_{\rm lab} < -2.5$[1] in the laboratory frame. The muon spectrometer consists of i) a front absorber made of carbon, concrete and steel of 10 nuclear interaction lengths

[1]The muon spectrometer covers a negative pseudo-rapidity range in the ALICE reference frame. η and y variables are experimentally identical for muons in the acceptance of the muon spectrometer and in pp collisions the physics results are symmetric with respect to η (y) = 0. They are presented as a function of y with positive values.

JHEP09(2019)008

($\lambda_{\rm I}$), located between the interaction point (IP) and the tracking system, that reduces the hadron yield and decreases the yield of muons from light-particle decays by limiting the free path of primary pions and kaons, ii) a beam shield throughout its entire length, iii) a dipole magnet with a field integral of 3 T·m, iv) five tracking stations, each composed of two planes of cathode pad chambers, v) two trigger stations, each equipped with two planes of resistive plate chambers and vi) an iron wall of 7.2 $\lambda_{\rm I}$ placed between the tracking and trigger systems, which absorbs secondary hadrons escaping from the front absorber as well as muons from light-hadron decays. In addition, the following detectors are also employed in the analysis. The Silicon Pixel Detector (SPD), which constitutes the two innermost layers of the Inner Tracking System, with pseudo-rapidity coverage $|\eta_{\rm lab}| < 2$ and $|\eta_{\rm lab}| < 1.4$ for the inner and outer layer, respectively, is used for reconstructing the position of the interaction vertex. Two scintillator arrays (V0) placed on each side of the IP, with pseudo-rapidity coverage $2.8 < \eta_{\rm lab} < 5.1$ and $-3.7 < \eta_{\rm lab} < -1.7$, are used for triggering purposes and to reject offline beam-induced background events. Finally, the two T0 arrays, made of quartz Cerenkov counters and placed on both sides of the IP, covering the acceptance $4.6 < \eta_{\rm lab} < 4.9$ and $-3.3 < \eta_{\rm lab} < -3.0$, are employed to determine the luminosity.

The results presented in this letter are based on the pp data sample at a centre-of-mass energy $\sqrt{s} = 5.02\,\text{TeV}$ recorded by ALICE during a short data taking period of five days in November 2015. This data sample consists of muon-triggered events requiring the coincidence of the minimum-bias (MB) trigger condition and at least one track segment in the muon trigger system with a $p_{\rm T}$ above the threshold of the online trigger algorithm. The MB trigger is formed by a coincidence between signals in the two V0 arrays. The samples of single muons were collected with the $p_{\rm T}$ threshold of the online trigger algorithm set to provide a 50% efficiency for muon tracks with either $p_{\rm T} \sim 0.5\,\text{GeV}/c$ or $p_{\rm T} \sim 4.2\,\text{GeV}/c$. In the following, the low- and high-$p_{\rm T}$ trigger threshold samples are referred to as MSL and MSH, respectively. Beam-gas interactions are reduced at the offline level using the timing information of the V0 detector. The accepted events have at least one interaction vertex reconstructed from hits correlation in the two SPD layers. The pile-up rate, defined as the probability for multiple interactions in a bunch crossing, was smaller than 2.5% during the whole data taking period and taken into account in the luminosity determination. After the event selection described above, the integrated luminosities for the used data samples are $\mathcal{L}_{\rm int} = 53.7 \pm 1.1\ \text{nb}^{-1}$ and $\mathcal{L}_{\rm int} = 104.4 \pm 2.2\ \text{nb}^{-1}$ for MSL- and MSH-triggered events, respectively. The calculation of the integrated luminosities and associated uncertainties is discussed in section 3.

3 Data analysis

3.1 Selection of muon candidates

Muon candidates are reconstructed using the algorithm described in [21]. They are further selected for the analysis applying same offline criteria as those described in [17, 18]. The muon identification is performed by requiring that the reconstructed track in the tracking system matches a track segment in the trigger system satisfying the trigger condition.

JHEP09(2019)008

Muon candidates are required to be reconstructed in the pseudo-rapidity region $-4 < \eta_{\rm lab} < -2.5$ and to have a polar angle measured at the end of the absorber in the interval $170^\circ < \theta_{\rm abs} < 178^\circ$. The $\theta_{\rm abs}$ condition allows us to limit multiple scattering by rejecting tracks passing through the high-density part of the front absorber. The contamination of fake tracks coming from the association of uncorrelated clusters in the tracking chambers and beam-induced background tracks is further reduced by applying a selection on the distance of the track to the primary vertex measured in the transverse plane (DCA, distance of closest approach) weighted with its momentum (p). The maximum value is set to $6\sigma_{p\cdot\rm DCA}$, where $\sigma_{p\cdot\rm DCA}$ is the resolution on this quantity. Finally, only muons with $p_{\rm T} > 2\,{\rm GeV}/c$ are analysed since according to Monte Carlo simulations [18], the contribution of muons from the decay of secondary light hadrons produced inside the front absorber is expected to be small in this region. The statistics recorded by ALICE allows us to perform the measurement of the production of muons from heavy-flavour hadron decays up to $p_{\rm T} = 20\,{\rm GeV}/c$ by combining MSL- and MSH-triggered events, which are used up to and above $p_{\rm T} = 7\,{\rm GeV}/c$, respectively. In the selected interval $2 < p_{\rm T} < 20\,{\rm GeV}/c$, the main remaining background contributions consist of muons from the decay of light (charged) hadrons (mostly pions and kaons) produced at the IP and muons from W and $\rm Z/\gamma^*$ decays, which dominate at low/intermediate $p_{\rm T}$ ($p_{\rm T} < 6$–$7\,{\rm GeV}/c$) and high $p_{\rm T}$ ($p_{\rm T} > 16$–$17\,{\rm GeV}/c$), respectively. Moreover, two additional background contributions, muons from secondary light (charged) hadron decays and muons from $\rm J/\psi$ decays, are also taken into account in the analysis, although they are small compared to the two other background sources.

3.2 Analysis procedure

The differential production cross section of muons from heavy-flavour hadron decays in a given $p_{\rm T}$ and y interval is computed as:

$$\frac{{\rm d}^2\sigma^{\mu^\pm\leftarrow{\rm HF}}}{{\rm d}p_{\rm T}{\rm d}y} = \frac{{\rm d}^2\sigma^{\mu^\pm}}{{\rm d}p_{\rm T}{\rm d}y} - \frac{{\rm d}^2\sigma^{\mu^\pm\leftarrow\pi}}{{\rm d}p_{\rm T}{\rm d}y} - \frac{{\rm d}^2\sigma^{\mu^\pm\leftarrow{\rm K}}}{{\rm d}p_{\rm T}{\rm d}y} - \frac{{\rm d}^2\sigma^{\mu^\pm\leftarrow{\rm sec.}\pi/{\rm K}}}{{\rm d}p_{\rm T}{\rm d}y} - \frac{{\rm d}^2\sigma^{\mu^\pm\leftarrow{\rm W/Z}/\gamma^*}}{{\rm d}p_{\rm T}{\rm d}y} - \frac{{\rm d}^2\sigma^{\mu^\pm\leftarrow{\rm J}/\psi}}{{\rm d}p_{\rm T}{\rm d}y}, \tag{3.1}$$

where ${\rm d}^2\sigma^{\mu^\pm}/{\rm d}p_{\rm T}{\rm d}y$ is the $p_{\rm T}$- and y-differential production cross section of inclusive muons and, ${\rm d}^2\sigma^{\mu^\pm\leftarrow\pi}/{\rm d}p_{\rm T}{\rm d}y$, ${\rm d}^2\sigma^{\mu^\pm\leftarrow{\rm K}}/{\rm d}p_{\rm T}{\rm d}y$, ${\rm d}^2\sigma^{\mu^\pm\leftarrow{\rm sec.}\pi/{\rm K}}/{\rm d}p_{\rm T}{\rm d}y$, ${\rm d}^2\sigma^{\mu^\pm\leftarrow{\rm W/Z}/\gamma^*}/{\rm d}p_{\rm T}{\rm d}y$ and ${\rm d}^2\sigma^{\mu^\pm\leftarrow{\rm J}/\psi}/{\rm d}p_{\rm T}{\rm d}y$ are the estimated $p_{\rm T}$- and y-differential production cross sections of muons from primary charged-pion decays, primary charged-kaon decays, secondary (charged) pion and kaon decays, W and $\rm Z/\gamma^*$ decays and $\rm J/\psi$ decays, respectively.

The inclusive muon production cross section is determined according to:

$$\frac{{\rm d}^2\sigma^{\mu^\pm}}{{\rm d}p_{\rm T}{\rm d}y} = \frac{1}{A\times\epsilon}\cdot\frac{{\rm d}^2N^{\mu^\pm}}{{\rm d}p_{\rm T}{\rm d}y}\cdot\frac{1}{\mathcal{L}_{\rm int}}, \tag{3.2}$$

where $A\times\epsilon$ is the product of acceptance and efficiency and ${\rm d}^2N^{\mu^\pm}/{\rm d}p_{\rm T}{\rm d}y$ is the measured $p_{\rm T}$- and y-differential muon yield. The integrated luminosity $\mathcal{L}_{\rm int}$ is computed as

JHEP09(2019)008

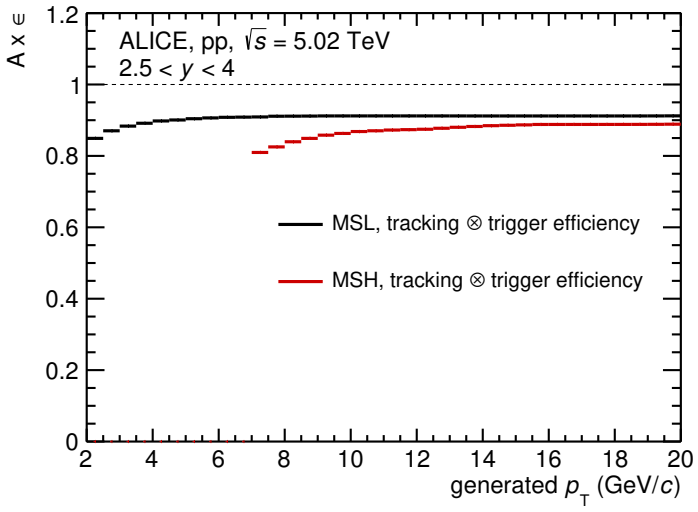

Figure 1. Product of acceptance and efficiency as a function of generated p_{T} estimated from a Monte Carlo simulation of muons from charm and beauty decays.

$N_{\mathrm{MSL(MSH)}}/\sigma_{\mathrm{MSL(MSH)}}$, where $N_{\mathrm{MSL(MSH)}}$ and $\sigma_{\mathrm{MSL(MSH)}}$ are the number of MSL (MSH)-triggered events and the corresponding MSL (MSH)-trigger cross section. The latter is expressed as $\sigma_{\mathrm{MSL(MSH)}} = \sigma_{\mathrm{T0}}/F_{\mathrm{MSL(MSH)}}$, where σ_{T0} and $F_{\mathrm{MSL(MSH)}}$ are the visible cross section for T0 measured with the van der Meer scan [22] and the corresponding normalisation factor. The T0 cross section amounts to $\sigma_{\mathrm{T0}} = 21.6 \pm 0.4$ mb. The total systematic uncertainty of 2.1% includes contributions from the T0 trigger cross section measurement and the stability of T0 during the data taking. The normalisation factors $F_{\mathrm{MSL}} = 34.30 \pm 0.05$ and $F_{\mathrm{MSH}} = 1370.9 \pm 2.2$ are the run-averaged ratio of T0 trigger rates corrected for pile-up to those of muon triggers (MSL or MSH) corrected by the fraction of events satisfying the event selection criteria. The quoted uncertainty is statistical, the systematic uncertainty being negligible (see section 3.3).

The measured p_{T}- and y-differential muon yields are corrected for the detector acceptance, tracking and trigger efficiencies ($A \times \epsilon$) using the same procedure as for previous analyses [17, 18, 23]. The $A \times \epsilon$ corrections are evaluated from Monte Carlo simulations where muons from charm and beauty decays[2] are generated using the input p_{T} and y distributions predicted by FONLL calculations [2]. These simulations are based on the GEANT3 transport code [24] for the detector description and response, and include the time evolution of the detector configuration as well as alignment effects. The resulting $A \times \epsilon$ in MSL-triggered events is almost independent of p_{T} and is about 90% for $p_{\mathrm{T}} > 4\,\mathrm{GeV}/c$, while in MSH-triggered events the $A \times \epsilon$ plateau is reached at higher p_{T}, about $15\,\mathrm{GeV}/c$ (figure 1).

The determination of the contribution of muons from charged pion and kaon decays, which dominates the background at low and intermediate p_{T}, is based on a data-tuned Monte Carlo cocktail. The procedure uses as inputs the p_{T}-differential mid-

[2]It was verified that the $A \times \epsilon$ correction is the same for all muons, disregarding their origin, within systematic uncertainties, in the considered kinematic region.

JHEP09(2019)008

rapidity yields of charged pions and kaons per inelastic pp collision at $\sqrt{s} = 5.02\,\text{TeV}$, $[\mathrm{d}^2N^{\pi^\pm(K^\pm)}/\mathrm{d}p_\mathrm{T}\mathrm{d}y]_{\mathrm{mid}-y}$, resulting from an interpolation of data measured in pp collisions at $\sqrt{s} = 2.76$ and 7 TeV, as described in [25–27]. These reference p_T spectra, measured up to $p_\mathrm{T} = 20\,\text{GeV}/c$, are extrapolated to higher p_T using a power-law fit to extend the p_T coverage to the p_T interval relevant for the estimation of the contribution of decay muons up to $p_\mathrm{T} = 20\,\text{GeV}/c$. Furthermore, the rapidity extrapolation of these distributions in a wider rapidity interval covering forward rapidities is performed according to:

$$\frac{\mathrm{d}^2N^{\pi^\pm(K^\pm)}}{\mathrm{d}p_\mathrm{T}\mathrm{d}y} = F_\mathrm{extrap}(p_\mathrm{T}, y) \cdot \left[\frac{\mathrm{d}^2N^{\pi^\pm(K^\pm)}}{\mathrm{d}p_\mathrm{T}\mathrm{d}y}\right]_{\mathrm{mid}-y}, \tag{3.3}$$

where $F_\mathrm{extrap}(p_\mathrm{T}, y)$ is the p_T-dependent rapidity extrapolation factor. The rapidity extrapolation is obtained from Monte Carlo simulations based on PYTHIA 6.4.25 [28] (Perugia-2011 [29]) and PHOJET [30] event generators. Furthermore, PYTHIA 8 [31] simulations with various colour reconnection (CR) options ("default MPI (Multi-Parton Interactions)", "new QCD" and "no CR") are employed to account for the p_T dependence of the rapidity extrapolation and to estimate the related systematic uncertainty. It was also checked that PYTHIA 8 [31] (Monash-2013 [32]) predictions give comparable results as PYTHIA 6 and PHOJET within uncertainties. Then, the p_T and y distributions of muons from the decay of charged pions and kaons are generated with a fast detector simulation of the decay kinematics and absorber effect, using as inputs the extrapolated primary charged pion and kaon spectra. The decay vertex of muons from charged pion and kaon decays is parameterised using either a single exponential for decays occurring before the front absorber ($z_\mathrm{v} \geq -90$ cm), or two exponentials for decays occurring inside the front absorber (-503 cm $< z_\mathrm{v} < -90$ cm), in which case the first exponential represents the decay probability whereas the second corresponds to the hadron absorption probability. The fraction of reconstructed muons produced after the front absorber is negligible. Finally, the yields are converted into a cross section and subtracted from the inclusive muon distribution. The relative contributions of muons from primary charged pion decays and muons from primary charged kaon decays to inclusive muons are comparable. In the acceptance of the muon spectrometer, $2.5 < y < 4$, the total contribution of muons from both charged pion and kaon decays decreases with increasing p_T from about 39% at $p_\mathrm{T} = 2\,\text{GeV}/c$ down to 4% at $p_\mathrm{T} = 20\,\text{GeV}/c$. This background contamination depends also on y, in particular at low p_T where it amounts to 47% and 26% in the rapidity intervals $2.5 < y < 2.8$ and $3.7 < y < 4$, respectively.

The contribution of muons from secondary (charged) pion and kaon decays resulting from the interaction of light-charged hadrons with the material of the front absorber of the ALICE muon spectrometer is estimated by means of simulations using PYTHIA 6.425 [28] and the GEANT3 transport code [24]. This contribution affects the low p_T region from $p_\mathrm{T} = 2\,\text{GeV}/c$ up to about $p_\mathrm{T} = 5$ GeV/c, only. The relative contribution with respect to inclusive muons decreases strongly with p_T, from about 4% at $p_\mathrm{T} = 2$ GeV/c to become smaller than 1% at $p_\mathrm{T} = 5$ GeV/c. It also varies with rapidity, by decreasing down to about 3% at $p_\mathrm{T} = 2$ GeV/c in the interval $3.7 < y < 4$.

JHEP09(2019)008

At high p_{T}, the W-boson decay muons and the dimuons from Z-boson decays and γ^* decays (Drell-Yan process) are the main contributions to the background muon p_{T} distribution. This background source is estimated with simulations using the POWHEG NLO event generator [33] paired with PYTHIA 6.425 [28] for parton shower simulation. These calculations use the CT10 PDFs [34]. The relative contribution of muons from W and Z/γ^* decays to the inclusive muon yield in $2.5 < y < 4$ is negligible for $p_{\mathrm{T}} < 12$ GeV/c and increases significantly with p_{T} from about 1% at $p_{\mathrm{T}} = 12$ GeV/c up to 12% in $18 < p_{\mathrm{T}} < 20$ GeV/c. It also depends on rapidity and varies as a function of rapidity in the range $3\% - 6\%$ in the interval $14 < p_{\mathrm{T}} < 20$ GeV/c.

The background component of muons from J/ψ decays is estimated by means of a data-driven method similar to that implemented for the evaluation of muons from primary charged pion and kaon decays. The procedure uses the inclusive J/ψ p_{T}- and y-differential cross sections measured by ALICE in the dimuon channel in the forward rapidity region ($2.5 < y < 4$) at $\sqrt{s} = 5.02$ TeV [35]. The J/ψ p_{T} distribution being limited to the interval $p_{\mathrm{T}} < 8$ GeV/c, it is fitted with the following function

$$f(p_{\mathrm{T}}) = C \cdot \frac{p_{\mathrm{T}}}{\left(1 + (\frac{p_{\mathrm{T}}}{p_0})^2\right)^n}, \tag{3.4}$$

where C, p_0 and n are free parameters, and further extrapolated to higher p_{T} values. The y distribution is also extended in a wider range by means of a second-order polynomial function in order to avoid edge effects. Finally, the contribution of muons from J/ψ decays is estimated with a simulation of the decay kinematics, using as inputs the extrapolated p_{T} and y production cross sections. As expected, this contamination is small compared to the other sources. The relative contribution with respect to the inclusive muon yield in the full acceptance of the muon spectrometer is maximum at intermediate p_{T} ($p_{\mathrm{T}} \sim 4$–6 GeV/c) where it amounts to about 4% and decreases with increasing p_{T} to become negligible for $p_{\mathrm{T}} > 15$ GeV/c (smaller than 1%). This background source exhibits a weak dependence on rapidity, with the maximum contribution at $p_{\mathrm{T}} \sim 4$–6 GeV/c varying within $4\% - 6\%$.

Figure 2 summarises the estimated relative contribution of the various sources of background with respect to inclusive muons as a function of p_{T} for the rapidity interval $2.5 < y < 4$, as well as the total background contamination. The vertical bars are the statistical uncertainties and the boxes are the systematic uncertainties on muon background sources that are discussed hereafter.

3.3 Systematic uncertainties

Several sources of systematic uncertainty affecting the measurement of the p_{T}- and y-differential production cross section of muons from heavy-flavour hadron decays are evaluated. These are the systematic uncertainties on the inclusive muon yield, the estimated background sources and the determination of the integrated luminosity.

The systematic uncertainty on the inclusive muon yield contains the following contributions. The systematic uncertainty on the muon tracking efficiency amounts to 0.5% and is estimated by measuring the efficiency in data and Monte Carlo with a procedure that exploits the redundancy of the tracking chamber information [20, 36]. The systematic

JHEP09(2019)008

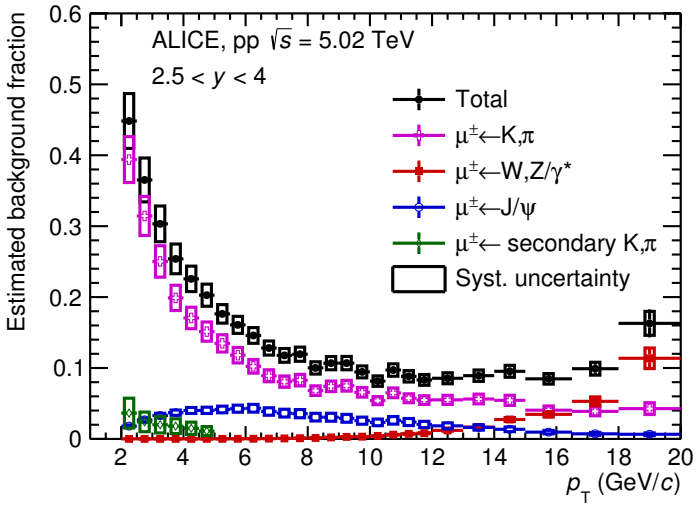

Figure 2. Estimated background fractions with respect to inclusive muons as a function of p_{T} for the rapidity interval $2.5 < y < 4$ in pp collisions at $\sqrt{s} = 5.02$ TeV. Statistical uncertainties (vertical bars) and systematic uncertainties (boxes) are shown.

uncertainty on the single muon trigger efficiency of 1.4% (3.2%) for MSL (MSH) trigger comes from the intrinsic efficiency of the trigger chambers and the response of the trigger algorithm. The first contribution is determined from the uncertainty on the trigger chamber efficiency measured in the data and applied to the simulations. The second one is estimated by comparing the p_{T} dependence of the MSL and MSH trigger response function in data and Monte Carlo [36]. A 0.5% contribution related to the choice of the χ^2 cut implemented for the matching between tracker and trigger tracks is also taken into account. The magnitude of these systematic uncertainties is approximately independent of the kinematics, in the region of interest. Finally, an additional contribution related to the tracking chamber resolution and alignment needs to be taken into account. The procedure employed for the estimation of this uncertainty is based on the one described in [37]. It uses a Monte Carlo simulation modelling the tracker response of the muon spectrometer with a parameterisation of the tracking chamber resolution and systematic mis-alignment effects. The former is measured using the residual distance between the reconstructed tracks and their associated clusters. The latter is inferred by comparing the reconstructed p_{T} distribution of positive and negative muons, which have opposite curvature in the dipole magnet field and thus opposite sensitivity to the mis-alignment. This parameterisation is tuned either on data or on the full Monte Carlo simulation. The comparison of the heavy-flavour decay muon p_{T}-differential distributions obtained with the two parameterisations gives an estimation of the systematic uncertainty. It is negligible for $p_{\mathrm{T}} < 7$ GeV/c and then increases to about 15% in the interval $18 < p_{\mathrm{T}} < 20$ GeV/c.

The systematic uncertainty on the estimated yield of muons from primary charged π (K) decays includes contributions from i) the measured mid-rapidity p_{T} distributions of charged π (K) up to $p_{\mathrm{T}} = 20$ GeV/c and their extrapolation to higher p_{T}, varying from about 7% (9%) to about 21% (22%) as a function of p_{T}, ii) the rapidity extrapolation of

JHEP09(2019)008

about 8.5% (6%) for muons from charged π (K), estimated by comparing the results with PYTHIA 6 and PHOJET generators iii) the p_{T} dependence of the rapidity extrapolation, negligible for $p_{\mathrm{T}} < 4$ GeV/c and increasing up to about 6% (3%) for charged π (K) decay muons, obtained by comparing the results with several colour reconnection options in PYTHIA 8 and iv) the simulation of hadronic interactions in the front absorber of about 4% for both charged π and K decay muons. The latter was estimated by comparing the p_{T} distributions of muons from charged pion and kaon decays obtained in a fast detector simulation based on a parameterisation of the effects of the front absorber (section 3.2) and a full simulation. Combining these sources, a total systematic uncertainty ranging from about 11% to 24% as a function of p_{T} is obtained, with approximately no dependence on the decay particle type. On the other hand, in order to account for the systematics associated to the transport code [18], a conservative systematic uncertainty on the estimated yield of muons from secondary charged π (K) decays of 100% is considered and the obtained difference between the upper and lower limits is further divided by $\sqrt{12}$, corresponding to one RMS of a uniform distribution.

The systematic uncertainty of the estimated yield of muons from W and Z/γ^* decays is determined by considering the CT10 PDF uncertainties. It amounts to about 8% (7%) for muons from W (Z/γ^*) decays.[3]

The systematic uncertainty on the extracted yield of muons from J/ψ originates from the measured J/ψ p_{T} and y distributions and their extrapolation in a wider kinematic region, with a negligible effect on the extracted muon yield when using different functions for the rapidity extrapolation. This systematic uncertainty increases with increasing p_{T} from about 10% to 34%.

The systematic uncertainty on the integrated luminosity reflects the 2.1% systematic uncertainty on the measurement of the T0 trigger cross section [22], the systematic uncertainty on the normalisation factor of muon-triggered events to the equivalent number of T0-triggered events based on the relative trigger rates being negligible. Indeed, compatible results are found when calculating the integrated luminosity for MSL (MSH) trigger by applying the corresponding trigger condition in the analysis of MB events, rather than using the relative trigger rates.

Table 1 gives an overview of the systematic uncertainties assigned to the various contributions which enter in the measurement of the p_{T}-differential cross section of muons from heavy-flavour hadron decays in $2.5 < y < 4$. The total systematic uncertainty is the quadratic sum of the sources listed in table 1, with the exception of the 2.1% contribution on the integrated luminosity which is fully correlated with p_{T}. It varies from about 2% to 15%, the smaller (higher) value corresponding to $p_{\mathrm{T}} = 6.5$ GeV/c ($18 < p_{\mathrm{T}} < 20$ GeV/c). In the high-p_{T} region ($18 < p_{\mathrm{T}} < 20$ GeV/c), the main contribution comes from the uncertainty on tracking chamber resolution and alignment.

4 Results and comparison with model predictions

The p_{T}-differential cross section of muons from heavy-flavour hadron decays in $2.5 < y < 4$ is presented in figure 3. The vertical bars represent the statistical uncertainties and are

[3] A similar systematic uncertainty is also obtained by performing POWHEG simulations with CTEQ6M (NLO) PDF [38].

JHEP09(2019)008

Source	Uncertainty vs p_{T}
Tracking efficiency	0.5%
Trigger efficiency	1.4% (3.2%) for MSL (MSH)
Matching efficiency	0.5%
Resolution and alignment	0–15% (negligible for $p_{\mathrm{T}} < 7$ GeV/c)
Background subtraction $\mu \leftarrow \pi$	1–4.4%
Background subtraction $\mu \leftarrow \mathrm{K}$	1–4.4%
Background subtraction $\mu \leftarrow$ sec. π, K	0–4.3%
Background subtraction $\mu \leftarrow W/Z/\gamma^*$	0–1.1%
Background subtraction $\mu \leftarrow \mathrm{J}/\psi$	0–0.7%
Integrated luminosity	2.1%

Table 1. Summary of relative systematic uncertainties after propagation to the measurement of the p_{T}-differential cross section of muons from heavy-flavour hadron decays at forward rapidity ($2.5 < y < 4$). See the text for details. For the p_{T}-dependent uncertainties, the minimum and maximum values are given. They are shown for the lowest and highest p_{T} interval with the exception of the light-hadron decay muon background, where this is the opposite trend, and of the background of muons from J/ψ decays with the maximum value being reached for $4 < p_{\mathrm{T}} < 6$ GeV/c. The systematic uncertainty on the integrated luminosity is correlated as a function of p_{T}.

smaller than the symbols in most p_{T} bins, while the empty boxes correspond to the systematic uncertainties. The symbols are positioned horizontally at the centre of each p_{T} bin and the horizontal bars represent the width of the p_{T} interval. These conventions are applied from here onwards to the figures discussed in the following. The measurement is carried out in a wider p_{T} range with respect to previous measurements in pp collisions [17, 18], the p_{T} reach being extended from $p_{\mathrm{T}} = 10$ GeV/c at $\sqrt{s} = 2.76$ TeV ($p_{\mathrm{T}} = 12$ GeV/c at $\sqrt{s} = 7$ TeV) to $p_{\mathrm{T}} = 20$ GeV/c by using MSL and MSH triggers. The total uncertainties (quadratic sum of statistical and systematic uncertainties) are reduced by a factor of about 2–4 with respect to previous measurements. These improvements have various sources: i) better understanding of the detector response, ii) new data-driven strategy for the estimation of the contribution of muons from light-hadron decays, iii) larger integrated luminosity and iv) use of a high-p_{T} trigger. The measured production cross section (figure 3, upper panel) is compared with FONLL predictions. The FONLL calculations [2, 6] include the non-perturbative fragmentation into open heavy-flavour hadrons and their decay into final-state leptons. As described in [39], the production of leptons from charm- and beauty-hadron decays is controlled by measured decay spectra and branching ratios. These predictions which use the CTEQ6.6 PDFs [40] are represented with a black curve and a shaded band for the systematic uncertainty. The latter contains the uncertainties on the renormalization and factorization scales, on quark masses as well as on the PDFs. The FONLL predictions are also displayed for muons coming from charm and beauty decays, separately. The latter contribution includes direct decays and decays via D-hadron decays. The FONLL predictions are compatible with data within the experimental and theoretical uncertainties. However, one can notice that the central values of FONLL predictions sys-

JHEP09(2019)008

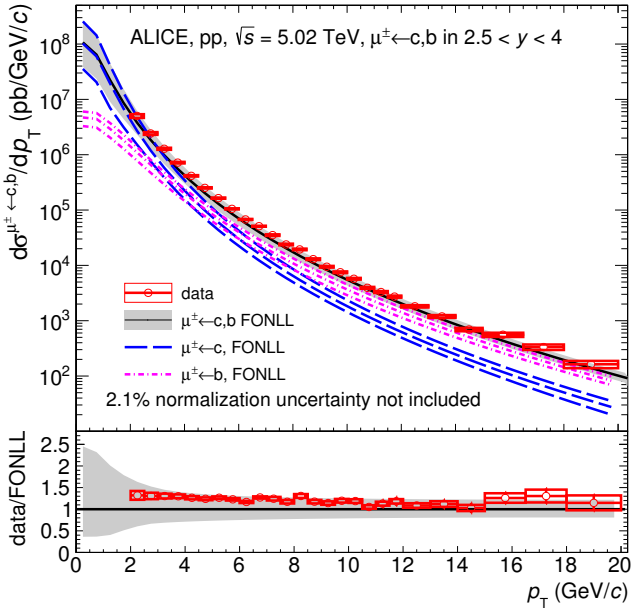

Figure 3. p_{T}-differential production cross section of muons from heavy-flavour hadron decays at forward rapidity in pp collisions at $\sqrt{s} = 5.02$ TeV. Statistical uncertainties (bars) and systematic uncertainties (boxes) are shown. The production cross section is compared with FONLL predictions [2] (top). The ratio of the data to FONLL calculations is shown in the lower panel. See the text for details.

tematically underestimate the measured production cross section at low and intermediate p_{T}, i.e. up to $p_{\mathrm{T}} \simeq 8$ GeV/c. This is also illustrated in the bottom panel of figure 3, which shows the ratio between the measured production cross section and the FONLL calculations. This ratio is about 1.3 for $2 < p_{\mathrm{T}} < 8$ GeV/c and then decreases with increasing p_{T} to tend towards unity in the high p_{T} region ($p_{\mathrm{T}} > 11$–12 GeV/c). Qualitatively, this behaviour was also reported at forward rapidity for muons from heavy-flavour hadron decays in previous analyses [17, 18] and for D mesons measured in pp collisions at $\sqrt{s} = 5.02$ and 13 TeV with the LHCb detector [15, 16], as well as at mid-rapidity for D mesons and electrons from B-hadron and heavy-flavour hadron decays measured in pp collisions at $\sqrt{s}$ = 2.76 and 7 TeV with ALICE [10, 13, 41–43].

The measurement described here provides the baseline for the study of QCD matter created in Pb-Pb collisions at the same centre-of-mass energy and in Xe-Xe collisions at $\sqrt{s_{\mathrm{NN}}} = 5.44$ TeV by applying a pQCD-driven energy scaling based on FONLL calculations [44].

The p_{T}-integrated production cross section of muons from heavy-flavour hadron decays is also studied as a function of rapidity for the p_{T} intervals $2 < p_{\mathrm{T}} < 7$ GeV/c and $7 < p_{\mathrm{T}} < 20$ GeV/c, as shown in left and right panels of figure 4, respectively. The ratios between data and FONLL predictions are depicted in the bottom panels. The two measurements are consistent with FONLL predictions. As in the case of the p_{T}-differential production cross section, the data lie in the upper part of the FONLL predictions. In the interval $2 < p_{\mathrm{T}} < 7$ GeV/c, muons from heavy-flavour hadron decays originate predominantly from

JHEP09(2019)008

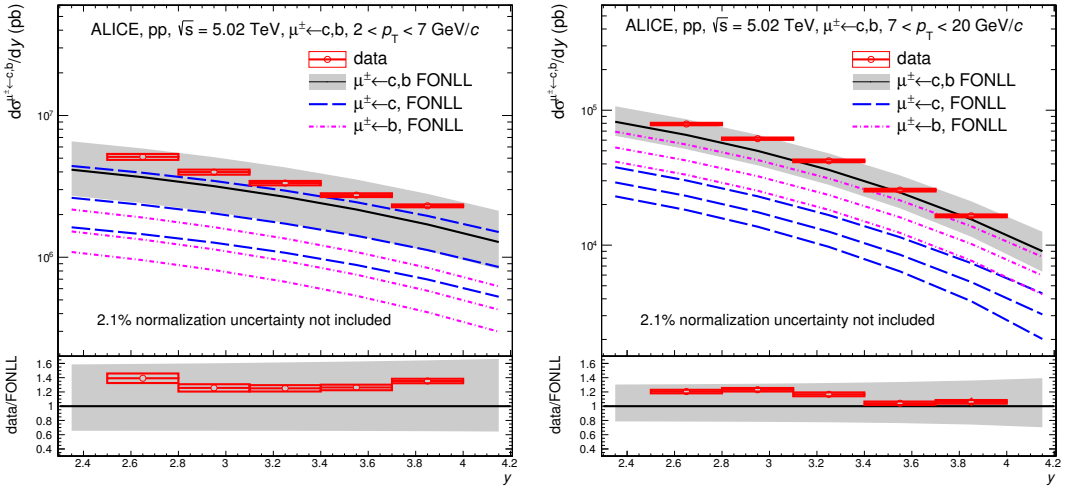

Figure 4. Production cross section of muons from heavy-flavour hadron decays as a function of rapidity in pp collisions at $\sqrt{s} = 5.02$ TeV for the p_{T} intervals $2 < p_{\mathrm{T}} < 7$ GeV/c (left) and $7 < p_{\mathrm{T}} < 20$ GeV/c (right). Statistical uncertainties (bars, smaller than symbols) and systematic uncertainties (boxes) are drawn. The production cross sections are compared with FONLL predictions [2] (top). The ratios of the data to FONLL calculations are shown in the lower panels. See the text for details.

charmed hadrons, while in the higher p_{T} region, muons from beauty-hadron decays take over from charm as the dominant source. One notices that in the higher p_{T} interval, the agreement between data and the central values of FONLL calculations is better. The ratio of the measured production cross section to FONLL predictions is in the range $\sim$ 1–1.2, depending on the rapidity region.

The statistics collected with muon triggers allows us to perform measurements of the p_{T}-differential cross section in five y intervals in the range $2.5 < y < 4$. The results and comparisons with FONLL are presented in figure 5, upper panel. The corresponding ratios between data and FONLL calculations are also displayed in figure 5, lower panel. The data and FONLL exhibit a good agreement within experimental and theoretical uncertainties, the former being systematically higher than the model calculations with some fluctuations at high p_{T}.

The ratio of open heavy-flavour production cross sections between different centre-of-mass energies is considered as a powerful observable for sensitive tests of pQCD-based calculations and to constrain gluon PDF at forward rapidity [6]. While the absolute production cross sections as predicted by FONLL are associated with large systematic uncertainties, dominated by the scale uncertainties, the ratios of production cross sections at different centre-of-mass energies are predicted with a better accuracy [6]. The ratio of the measured p_{T}-differential cross section of muons from heavy-flavour hadron decays in pp collisions at $\sqrt{s} = 7$ TeV to that at $\sqrt{s} = 5.02$ TeV in the rapidity interval $2.5 < y < 4$ is reported in figure 6. The systematic uncertainties between the two measurements are considered as uncorrelated when forming the ratio and the main contribution comes from the measurement at $\sqrt{s} = 7$ TeV. The ratio exhibits a smooth increase with increasing p_{T} from about 1.5 ($p_{\mathrm{T}} = 2$ GeV/c) to 1.8 ($p_{\mathrm{T}} = 12$ GeV/c). The data are compared with FONLL predictions [2]. The measured ratio is well reproduced by FONLL calculations.

JHEP09(2019)008

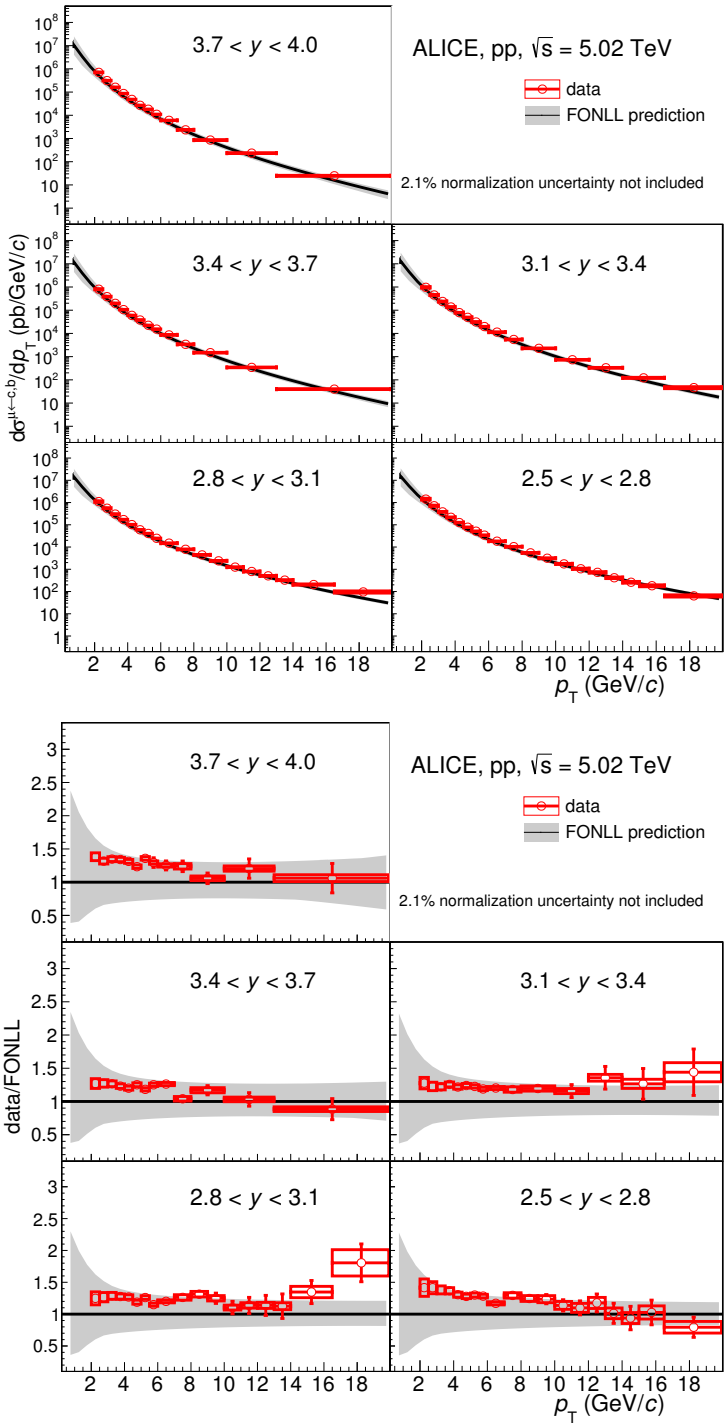

Figure 5. Upper panel: p_{T}-differential production cross section of muons from heavy-flavour hadron decays for five rapidity intervals in the range $2.5 < y < 4$ in pp collisions at $\sqrt{s} = 5.02$ TeV. Statistical uncertainties (bars) and systematic uncertainties (boxes) are shown. The production cross sections are compared with FONLL predictions [2]. Bottom panel: ratios of the data to FONLL calculations. See the text for details.

JHEP09(2019)008

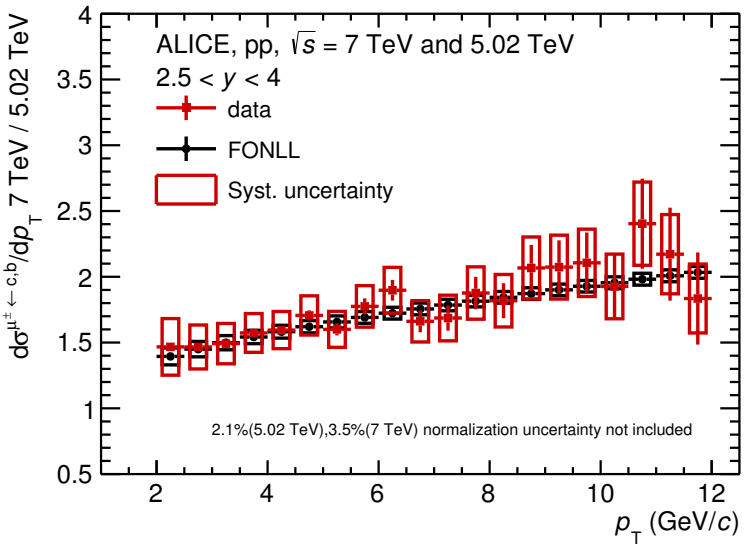

Figure 6. Ratio of the p_{T}-differential production cross section of muons from heavy-flavour hadron decays at forward rapidity in pp collisions at $\sqrt{s} = 7$ TeV to that at $\sqrt{s} = 5.02$ TeV. Statistical uncertainties (bars) and systematic uncertainties (boxes) are shown. The normalisation uncertainty contains the uncertainties on the luminosity at the two centre-of-mass energies. The ratio is compared with FONLL predictions [2]. See the text for details.

A reduction of the systematic uncertainty on the FONLL predictions is also expected from the ratio of open heavy-flavour cross sections between different rapidity intervals, which could provide constraints on the gluon PDF at small Bjorken-x values. This ratio, computed for heavy-flavour hadron decay muons between the two extreme rapidity intervals, i.e. $2.5 < y < 2.8$ and $3.7 < y < 4$, is presented in figure 7. When forming the ratio, the systematic uncertainty on integrated luminosity is correlated, while the systematic uncertainty on tracking chamber resolution and alignment is partially correlated. The other sources of systematic uncertainties are treated as uncorrelated. The ratio decreases significantly with increasing p_{T} from about 0.5 down to 0.15. The measured ratio is compared with FONLL predictions, which describe the data within their uncertainties.

5 Conclusions

In summary, the production of muons from heavy-flavour hadron decays has been measured in the forward rapidity region as a function of p_{T} and y in pp collisions at $\sqrt{s} = 5.02$ TeV with the ALICE detector at the CERN LHC. As compared to previously published measurements, the present results have an extended p_{T} coverage, $2 < p_{\mathrm{T}} < 20$ GeV/c, and a better precision with the total uncertainties reduced by a factor of about 2–4, depending on p_{T}. The results provide the crucial reference for the study of the effects of the hot and dense matter on the production of muons from heavy-flavour hadron decays in Pb-Pb collisions at the same centre-of-mass energy. The measurements of the differential production cross sections are found to be in agreement with FONLL predictions over the full p_{T} range, even though the central values of FONLL appear to underestimate the heavy-flavour hadron

JHEP09(2019)008

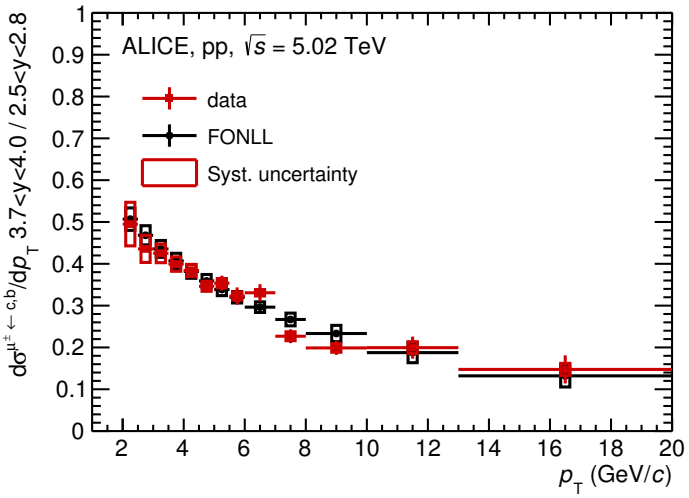

Figure 7. Ratio of the p_{T}-differential production cross section of muons from heavy-flavour hadron decays in $3.7 < y < 4$ to that in $2.5 < y < 2.8$ in pp collisions at $\sqrt{s} = 5.02$ TeV. Statistical uncertainties (bars) and systematic uncertainties (boxes) are shown. The ratio is compared with FONLL predictions [2]. See the text for details.

decay muon production. The p_{T}-differential ratios of the production cross section between $\sqrt{s} = 7$ TeV and $\sqrt{s} = 5.02$ TeV and between two rapidity intervals within $2.5 < y < 4$ are well described by FONLL calculations.

Acknowledgments

The ALICE Collaboration would like to thank all its engineers and technicians for their invaluable contributions to the construction of the experiment and the CERN accelerator teams for the outstanding performance of the LHC complex. The ALICE Collaboration gratefully acknowledges the resources and support provided by all Grid centres and the Worldwide LHC Computing Grid (WLCG) collaboration. The ALICE Collaboration acknowledges the following funding agencies for their support in building and running the ALICE detector: A. I. Alikhanyan National Science Laboratory (Yerevan Physics Institute) Foundation (ANSL), State Committee of Science and World Federation of Scientists (WFS), Armenia; Austrian Academy of Sciences, Austrian Science Fund (FWF): [M 2467-N36] and Nationalstiftung für Forschung, Technologie und Entwicklung, Austria; Ministry of Communications and High Technologies, National Nuclear Research Center, Azerbaijan; Conselho Nacional de Desenvolvimento Científico e Tecnológico (CNPq), Universidade Federal do Rio Grande do Sul (UFRGS), Financiadora de Estudos e Projetos (Finep) and Fundação de Amparo à Pesquisa do Estado de São Paulo (FAPESP), Brazil; Ministry of Science & Technology of China (MSTC), National Natural Science Foundation of China (NSFC) and Ministry of Education of China (MOEC), China; Croatian Science Foundation and Ministry of Science and Education, Croatia; Centro de Aplicaciones Tecnológicas y Desarrollo Nuclear (CEADEN), Cubaenergía, Cuba; Ministry of Education, Youth and Sports of the Czech Republic, Czech Republic; The Danish Council for In-

JHEP09(2019)008

dependent Research — Natural Sciences, the Carlsberg Foundation and Danish National Research Foundation (DNRF), Denmark; Helsinki Institute of Physics (HIP), Finland; Commissariat à l'Energie Atomique (CEA), Institut National de Physique Nucléaire et de Physique des Particules (IN2P3) and Centre National de la Recherche Scientifique (CNRS) and Région des Pays de la Loire, France; Bundesministerium für Bildung und Forschung (BMBF) and GSI Helmholtzzentrum für Schwerionenforschung GmbH, Germany; General Secretariat for Research and Technology, Ministry of Education, Research and Religions, Greece; National Research, Development and Innovation Office, Hungary; Department of Atomic Energy Government of India (DAE), Department of Science and Technology, Government of India (DST), University Grants Commission, Government of India (UGC) and Council of Scientific and Industrial Research (CSIR), India; Indonesian Institute of Science, Indonesia; Centro Fermi — Museo Storico della Fisica e Centro Studi e Ricerche Enrico Fermi and Istituto Nazionale di Fisica Nucleare (INFN), Italy; Institute for Innovative Science and Technology , Nagasaki Institute of Applied Science (IIST), Japan Society for the Promotion of Science (JSPS) KAKENHI and Japanese Ministry of Education, Culture, Sports, Science and Technology (MEXT), Japan; Consejo Nacional de Ciencia (CONACYT) y Tecnología, through Fondo de Cooperación Internacional en Ciencia y Tecnología (FONCICYT) and Dirección General de Asuntos del Personal Academico (DGAPA), Mexico; Nederlandse Organisatie voor Wetenschappelijk Onderzoek (NWO), Netherlands; The Research Council of Norway, Norway; Commission on Science and Technology for Sustainable Development in the South (COMSATS), Pakistan; Pontificia Universidad Católica del Perú, Peru; Ministry of Science and Higher Education and National Science Centre, Poland; Korea Institute of Science and Technology Information and National Research Foundation of Korea (NRF), Republic of Korea; Ministry of Education and Scientific Research, Institute of Atomic Physics and Ministry of Research and Innovation and Institute of Atomic Physics, Romania; Joint Institute for Nuclear Research (JINR), Ministry of Education and Science of the Russian Federation, National Research Centre Kurchatov Institute, Russian Science Foundation and Russian Foundation for Basic Research, Russia; Ministry of Education, Science, Research and Sport of the Slovak Republic, Slovakia; National Research Foundation of South Africa, South Africa; Swedish Research Council (VR) and Knut & Alice Wallenberg Foundation (KAW), Sweden; European Organization for Nuclear Research, Switzerland; National Science and Technology Development Agency (NSDTA), Suranaree University of Technology (SUT) and Office of the Higher Education Commission under NRU project of Thailand, Thailand; Turkish Atomic Energy Agency (TAEK), Turkey; National Academy of Sciences of Ukraine, Ukraine; Science and Technology Facilities Council (STFC), United Kingdom; National Science Foundation of the United States of America (NSF) and United States Department of Energy, Office of Nuclear Physics (DOE NP), United States of America.

JHEP09(2019)008

References

[1] M. Cacciari, M. Greco and P. Nason, *The p_T spectrum in heavy flavor hadroproduction*, *JHEP* **05** (1998) 007 [hep-ph/9803400] [INSPIRE].

[2] M. Cacciari et al., *Theoretical predictions for charm and bottom production at the LHC*, *JHEP* **10** (2012) 137 [arXiv:1205.6344] [INSPIRE].

[3] B.A. Kniehl, *Inclusive production of heavy-flavored hadrons at NLO in the GM-VFNS*, in the proceedings of the 16th *International Workshop on Deep Inelastic Scattering and Related Subjects (DIS 2008)*, April 7–11, London, U.K. (2008), arXiv:0807.2215 [INSPIRE].

[4] B.A. Kniehl, G. Kramer, I. Schienbein and H. Spiesberger, *Inclusive B-meson production at the LHC in the GM-VFN scheme*, *Phys. Rev.* **D 84** (2011) 094026 [arXiv:1109.2472] [INSPIRE].

[5] R. Maciula and A. Szczurek, *Charmed mesons and leptons from semileptonic decays at the LHC*, PoS(DIS 2013)169 [arXiv:1306.6808] [INSPIRE].

[6] M. Cacciari, M.L. Mangano and P. Nason, *Gluon PDF constraints from the ratio of forward heavy-quark production at the LHC at $\sqrt{s} = 7$ and 13 TeV*, *Eur. Phys. J.* **C 75** (2015) 610 [arXiv:1507.06197] [INSPIRE].

[7] A. Andronic et al., *Heavy-flavour and quarkonium production in the LHC era: from proton–proton to heavy-ion collisions*, *Eur. Phys. J.* **C 76** (2016) 107 [arXiv:1506.03981] [INSPIRE].

[8] CMS collaboration, *Measurement of the total and differential inclusive B^+ hadron cross sections in pp collisions at $\sqrt{s} = 13$ TeV*, *Phys. Lett.* **B 771** (2017) 435 [arXiv:1609.00873] [INSPIRE].

[9] ALICE collaboration, *Measurements of low-p_T electrons from semileptonic heavy-flavour hadron decays at mid-rapidity in pp and Pb-Pb collisions at $\sqrt{s_{\rm NN}} = 2.76$ TeV*, *JHEP* **10** (2018) 061 [arXiv:1805.04379] [INSPIRE].

[10] ALICE collaboration, *Measurement of electrons from beauty hadron decays in pp collisions at $\sqrt{s} = 7$ TeV*, *Phys. Lett.* **B 721** (2013) 13 [*Erratum ibid.* **B 763** (2016) 507] [arXiv:1208.1902] [INSPIRE].

[11] ALICE collaboration, *Λ_c^+ production in pp collisions at $\sqrt{s} = 7$ TeV and in p-Pb collisions at $\sqrt{s_{NN}} = 5.02$ TeV*, *JHEP* **04** (2018) 108 [arXiv:1712.09581] [INSPIRE].

[12] ALICE collaboration, *First measurement of Ξ_c^0 production in pp collisions at $\sqrt{s} = 7$ TeV*, *Phys. Lett.* **B 781** (2018) 8 [arXiv:1712.04242] [INSPIRE].

[13] ALICE collaboration, *Measurement of D-meson production at mid-rapidity in pp collisions at $\sqrt{s} = 7$ TeV*, *Eur. Phys. J.* **C 77** (2017) 550 [arXiv:1702.00766] [INSPIRE].

[14] ALICE collaboration, *D-meson production in p-Pb collisions at $\sqrt{s_{NN}} = 5.02$ TeV and in pp collisions at $\sqrt{s} = 7$ TeV*, *Phys. Rev.* **C 94** (2016) 054908 [arXiv:1605.07569] [INSPIRE].

[15] LHCb collaboration, *Measurements of prompt charm production cross-sections in pp collisions at $\sqrt{s} = 13$ TeV*, *JHEP* **03** (2016) 159 [*Erratum ibid.* **09** (2016) 013] [arXiv:1510.01707] [INSPIRE].

[16] LHCb collaboration, *Measurements of prompt charm production cross-sections in pp collisions at $\sqrt{s} = 5$ TeV*, *JHEP* **06** (2017) 147 [arXiv:1610.02230] [INSPIRE].

JHEP09(2019)008

[17] ALICE collaboration, *Production of muons from heavy flavour decays at forward rapidity in pp and Pb-Pb collisions at* $\sqrt{s_{NN}} = 2.76$ *TeV*, *Phys. Rev. Lett.* **109** (2012) 112301 [arXiv:1205.6443] [INSPIRE].

[18] ALICE collaboration, *Heavy flavour decay muon production at forward rapidity in proton–proton collisions at* $\sqrt{s} = 7$ *TeV*, *Phys. Lett.* **B 708** (2012) 265 [arXiv:1201.3791] [INSPIRE].

[19] ALICE collaboration, *The ALICE experiment at the CERN LHC*, 2008 *JINST* **3** S08002 [INSPIRE].

[20] ALICE collaboration, *Performance of the ALICE experiment at the CERN LHC*, *Int. J. Mod. Phys.* **A 29** (2014) 1430044 [arXiv:1402.4476] [INSPIRE].

[21] ALICE collaboration, *Rapidity and transverse momentum dependence of inclusive* J/ψ *production in pp collisions at* $\sqrt{s} = 7$ *TeV*, *Phys. Lett.* **B 704** (2011) 442 [*Erratum ibid.* **B 718** (2012) 692] [arXiv:1105.0380] [INSPIRE].

[22] ALICE collaboration, *ALICE luminosity determination for pp collisions at* $\sqrt{s} = 5$ *TeV*, ALICE-PUBLIC-2016-005 (2016) .

[23] ALICE collaboration, *Production of muons from heavy-flavour hadron decays in p-Pb collisions at* $\sqrt{s_{NN}} = 5.02$ *TeV*, *Phys. Lett.* **B 770** (2017) 459 [arXiv:1702.01479] [INSPIRE].

[24] R. Brun et al., *GEANT detector description and simulation tool*, CERN-W5013 (1994).

[25] ALICE collaboration, *Production of charged pions, kaons and protons at large transverse momenta in pp and Pb–Pb collisions at* $\sqrt{s_{NN}} = 2.76$ *TeV*, *Phys. Lett.* **B 736** (2014) 196 [arXiv:1401.1250] [INSPIRE].

[26] ALICE collaboration, *Measurement of pion, kaon and proton production in proton–proton collisions at* $\sqrt{s} = 7$ *TeV*, *Eur. Phys. J.* **C 75** (2015) 226 [arXiv:1504.00024] [INSPIRE].

[27] ALICE collaboration, *Multiplicity dependence of charged pion, kaon and (anti)proton production at large transverse momentum in p-Pb collisions at* $\sqrt{s_{NN}} = 5.02$ *TeV*, *Phys. Lett.* **B 760** (2016) 720 [arXiv:1601.03658] [INSPIRE].

[28] T. Sjöstrand, S. Mrenna and P.Z. Skands, *PYTHIA 6.4 physics and manual*, *JHEP* **05** (2006) 026 [hep-ph/0603175] [INSPIRE].

[29] P.Z. Skands, *Tuning Monte Carlo generators: the Perugia tunes*, *Phys. Rev.* **D 82** (2010) 074018 [arXiv:1005.3457] [INSPIRE].

[30] R. Engel, J. Ranft and S. Roesler, *Hard diffraction in hadron-hadron interactions and in photoproduction*, *Phys. Rev.* **D 52** (1995) 1459.

[31] T. Sjöstrand et al., *An introduction to PYTHIA 8.2*, *Comput. Phys. Commun.* **191** (2015) 159 [arXiv:1410.3012] [INSPIRE].

[32] P. Skands, S. Carrazza and J. Rojo, *Tuning PYTHIA 8.1: the Monash 2013 Tune*, *Eur. Phys. J.* **C 74** (2014) 3024 [arXiv:1404.5630] [INSPIRE].

[33] S. Alioli, P. Nason, C. Oleari and E. Re, *NLO vector-boson production matched with shower in POWHEG*, *JHEP* **07** (2008) 060 [arXiv:0805.4802] [INSPIRE].

[34] H.-L. Lai et al., *New parton distributions for collider physics*, *Phys. Rev.* **D 82** (2010) 074024 [arXiv:1007.2241] [INSPIRE].

JHEP09(2019)008

[35] ALICE collaboration, *Energy dependence of forward-rapidity J/ψ and $\psi(2S)$ production in pp collisions at the LHC*, *Eur. Phys. J.* **C 77** (2017) 392 [arXiv:1702.00557] [INSPIRE].

[36] ALICE collaboration, *Differential studies of inclusive J/ψ and $\psi(2S)$ production at forward rapidity in Pb-Pb collisions at $\sqrt{s_{NN}} = 2.76$ TeV*, *JHEP* **05** (2016) 179 [arXiv:1506.08804] [INSPIRE].

[37] ALICE collaboration, *W and Z boson production in p-Pb collisions at $\sqrt{s_{NN}} = 5.02$ TeV*, *JHEP* **02** (2017) 077 [arXiv:1611.03002] [INSPIRE].

[38] J. Pumplin et al., *New generation of parton distributions with uncertainties from global QCD analysis*, *JHEP* **07** (2002) 012 [hep-ph/0201195] [INSPIRE].

[39] M. Cacciari, P. Nason and R. Vogt, *QCD predictions for charm and bottom production at RHIC*, *Phys. Rev. Lett.* **95** (2005) 122001 [hep-ph/0502203] [INSPIRE].

[40] P.M. Nadolsky et al., *Implications of CTEQ global analysis for collider observables*, *Phys. Rev.* **D 78** (2008) 013004 [arXiv:0802.0007] [INSPIRE].

[41] ALICE collaboration, *Beauty production in pp collisions at $\sqrt{s} = 2.76$ TeV measured via semi-electronic decays*, *Phys. Lett.* **B 738** (2014) 97 [arXiv:1405.4144] [INSPIRE].

[42] ALICE collaboration, *Measurement of electrons from semileptonic heavy-flavor hadron decays in pp collisions at $\sqrt{s} = 2.76$ TeV*, *Phys. Rev.* **D 91** (2015) 012001 [arXiv:1405.4117] [INSPIRE].

[43] ALICE collaboration, *Measurement of charm production at central rapidity in proton-proton collisions at $\sqrt{s} = 2.76$ TeV*, *JHEP* **07** (2012) 191 [arXiv:1205.4007] [INSPIRE].

[44] R. Averbeck et al., *Reference heavy flavour cross sections in pp collisions at $\sqrt{s} = 2.76$ TeV, using a pQCD-Driven $\sqrt{s}$-scaling of ALICE measurements at $\sqrt{s} = 7$ TeV*, arXiv:1107.3243 [INSPIRE].

JHEP09(2019)008

The ALICE collaboration

S. Acharya[141], D. Adamová[93], S.P. Adhya[141], A. Adler[74], J. Adolfsson[80], M.M. Aggarwal[98], G. Aglieri Rinella[34], M. Agnello[31], N. Agrawal[10], Z. Ahammed[141], S. Ahmad[17], S.U. Ahn[76], S. Aiola[146], A. Akindinov[64], M. Al-Turany[105], S.N. Alam[141], D.S.D. Albuquerque[122], D. Aleksandrov[87], B. Alessandro[58], H.M. Alfanda[6], R. Alfaro Molina[72], B. Ali[17], Y. Ali[15], A. Alici[10,53,27], A. Alkin[2], J. Alme[22], T. Alt[69], L. Altenkamper[22], I. Altsybeev[112], M.N. Anaam[6], C. Andrei[47], D. Andreou[34], H.A. Andrews[109], A. Andronic[144], M. Angeletti[34], V. Anguelov[102], C. Anson[16], T. Antičić[106], F. Antinori[56], P. Antonioli[53], R. Anwar[126], N. Apadula[79], L. Aphecetche[114], H. Appelshäuser[69], S. Arcelli[27], R. Arnaldi[58], M. Arratia[79], I.C. Arsene[21], M. Arslandok[102], A. Augustinus[34], R. Averbeck[105], S. Aziz[61], M.D. Azmi[17], A. Badalà[55], Y.W. Baek[40], S. Bagnasco[58], R. Bailhache[69], R. Bala[99], A. Baldisseri[137], M. Ball[42], R.C. Baral[85], R. Barbera[28], L. Barioglio[26], G.G. Barnaföldi[145], L.S. Barnby[92], V. Barret[134], P. Bartalini[6], K. Barth[34], E. Bartsch[69], F. Baruffaldi[29], N. Bastid[134], S. Basu[143], G. Batigne[114], B. Batyunya[75], P.C. Batzing[21], D. Bauri[48], J.L. Bazo Alba[110], I.G. Bearden[88], C. Bedda[63], N.K. Behera[60], I. Belikov[136], F. Bellini[34], R. Bellwied[126], V. Belyaev[91], G. Bencedi[145], S. Beole[26], A. Bercuci[47], Y. Berdnikov[96], D. Berenyi[145], R.A. Bertens[130], D. Berzano[58], L. Betev[34], A. Bhasin[99], I.R. Bhat[99], H. Bhatt[48], B. Bhattacharjee[41], A. Bianchi[26], L. Bianchi[126,26], N. Bianchi[51], J. Bielčík[37], J. Bielčíková[93], A. Bilandzic[103,117], G. Biro[145], R. Biswas[3], S. Biswas[3], J.T. Blair[119], D. Blau[87], C. Blume[69], G. Boca[139], F. Bock[34,94], A. Bogdanov[91], L. Boldizsár[145], A. Bolozdynya[91], M. Bombara[38], G. Bonomi[140], M. Bonora[34], H. Borel[137], A. Borissov[144,91], M. Borri[128], H. Bossi[146], E. Botta[26], C. Bourjau[88], L. Bratrud[69], P. Braun-Munzinger[105], M. Bregant[121], T.A. Broker[69], M. Broz[37], E.J. Brucken[43], E. Bruna[58], G.E. Bruno[33,104], M.D. Buckland[128], D. Budnikov[107], H. Buesching[69], S. Bufalino[31], O. Bugnon[114], P. Buhler[113], P. Buncic[34], O. Busch[133,i], Z. Buthelezi[73], J.B. Butt[15], J.T. Buxton[95], D. Caffarri[89], A. Caliva[105], E. Calvo Villar[110], R.S. Camacho[44], P. Camerini[25], A.A. Capon[113], F. Carnesecchi[10], J. Castillo Castellanos[137], A.J. Castro[130], E.A.R. Casula[54], F. Catalano[31], C. Ceballos Sanchez[52], P. Chakraborty[48], S. Chandra[141], B. Chang[127], W. Chang[6], S. Chapeland[34], M. Chartier[128], S. Chattopadhyay[141], S. Chattopadhyay[108], A. Chauvin[24], C. Cheshkov[135], B. Cheynis[135], V. Chibante Barroso[34], D.D. Chinellato[122], S. Cho[60], P. Chochula[34], T. Chowdhury[134], P. Christakoglou[89], C.H. Christensen[88], P. Christiansen[80], T. Chujo[133], C. Cicalo[54], L. Cifarelli[10,27], F. Cindolo[53], J. Cleymans[125], F. Colamaria[52], D. Colella[52], A. Collu[79], M. Colocci[27], M. Concas[58,ii], G. Conesa Balbastre[78], Z. Conesa del Valle[61], G. Contin[128], J.G. Contreras[37], T.M. Cormier[94], Y. Corrales Morales[26,58], P. Cortese[32], M.R. Cosentino[123], F. Costa[34], S. Costanza[139], J. Crkovská[61], P. Crochet[134], E. Cuautle[70], L. Cunqueiro[94], D. Dabrowski[142], T. Dahms[103,117], A. Dainese[56], F.P.A. Damas[137,114], S. Dani[66], M.C. Danisch[102], A. Danu[68], D. Das[108], I. Das[108], S. Das[3], A. Dash[85], S. Dash[48], A. Dashi[103], S. De[85,49], A. De Caro[30], G. de Cataldo[52], C. de Conti[121], J. de Cuveland[39], A. De Falco[24], D. De Gruttola[10], N. De Marco[58], S. De Pasquale[30], R.D. De Souza[122], S. Deb[49], H.F. Degenhardt[121], A. Deisting[102,105], K.R. Deja[142], A. Deloff[84], S. Delsanto[131,26], P. Dhankher[48], D. Di Bari[33], A. Di Mauro[34], R.A. Diaz[8], T. Dietel[125], P. Dillenseger[69], Y. Ding[6], R. Divià[34], Ø. Djuvsland[22], U. Dmitrieva[62], A. Dobrin[34,68], B. Dönigus[69], O. Dordic[21], A.K. Dubey[141], A. Dubla[105], S. Dudi[98], A.K. Duggal[98], M. Dukhishyam[85], P. Dupieux[134], R.J. Ehlers[146], D. Elia[52], H. Engel[74], E. Epple[146], B. Erazmus[114], F. Erhardt[97], A. Erokhin[112], M.R. Ersdal[22], B. Espagnon[61], G. Eulisse[34], J. Eum[18], D. Evans[109], S. Evdokimov[90], L. Fabbietti[117,103], M. Faggin[29], J. Faivre[78], A. Fantoni[51], M. Fasel[94], P. Fecchio[31], L. Feldkamp[144], A. Feliciello[58], G. Feofilov[112], A. Fernández Téllez[44], A. Ferrero[137], A. Ferretti[26], A. Festanti[34], V.J.G. Feuillard[102], J. Figiel[118], S. Filchagin[107], D. Finogeev[62], F.M. Fionda[22], G. Fiorenza[52], F. Flor[126], S. Foertsch[73],

JHEP09(2019)008

P. Foka[105], S. Fokin[87], E. Fragiacomo[59], A. Francisco[114], U. Frankenfeld[105], G.G. Fronze[26], U. Fuchs[34], C. Furget[78], A. Furs[62], M. Fusco Girard[30], J.J. Gaardhøje[88], M. Gagliardi[26], A.M. Gago[110], A. Gal[136], C.D. Galvan[120], P. Ganoti[83], C. Garabatos[105], E. Garcia-Solis[11], K. Garg[28], C. Gargiulo[34], K. Garner[144], P. Gasik[103,117], E.F. Gauger[119], M.B. Gay Ducati[71], M. Germain[114], J. Ghosh[108], P. Ghosh[141], S.K. Ghosh[3], P. Gianotti[51], P. Giubellino[105,58], P. Giubilato[29], P. Glässel[102], D.M. Goméz Coral[72], A. Gomez Ramirez[74], V. Gonzalez[105], P. González-Zamora[44], S. Gorbunov[39], L. Görlich[118], S. Gotovac[35], V. Grabski[72], L.K. Graczykowski[142], K.L. Graham[109], L. Greiner[79], A. Grelli[63], C. Grigoras[34], V. Grigoriev[91], A. Grigoryan[1], S. Grigoryan[75], O.S. Groettvik[22], J.M. Gronefeld[105], F. Grosa[31], J.F. Grosse-Oetringhaus[34], R. Grosso[105], R. Guernane[78], B. Guerzoni[27], M. Guittiere[114], K. Gulbrandsen[88], T. Gunji[132], A. Gupta[99], R. Gupta[99], I.B. Guzman[44], R. Haake[146,34], M.K. Habib[105], C. Hadjidakis[61], H. Hamagaki[81], G. Hamar[145], M. Hamid[6], J.C. Hamon[136], R. Hannigan[119], M.R. Haque[63], A. Harlenderova[105], J.W. Harris[146], A. Harton[11], H. Hassan[78], D. Hatzifotiadou[10,53], P. Hauer[42], S. Hayashi[132], S.T. Heckel[69], E. Hellbär[69], H. Helstrup[36], A. Herghelegiu[47], E.G. Hernandez[44], G. Herrera Corral[9], F. Herrmann[144], K.F. Hetland[36], T.E. Hilden[43], H. Hillemanns[34], C. Hills[128], B. Hippolyte[136], B. Hohlweger[103], D. Horak[37], S. Hornung[105], R. Hosokawa[133], P. Hristov[34], C. Huang[61], C. Hughes[130], P. Huhn[69], T.J. Humanic[95], H. Hushnud[108], L.A. Husova[144], N. Hussain[41], S.A. Hussain[15], T. Hussain[17], D. Hutter[39], D.S. Hwang[19], J.P. Iddon[128], R. Ilkaev[107], M. Inaba[133], M. Ippolitov[87], M.S. Islam[108], M. Ivanov[105], V. Ivanov[96], V. Izucheev[90], B. Jacak[79], N. Jacazio[27], P.M. Jacobs[79], M.B. Jadhav[48], S. Jadlovska[116], J. Jadlovsky[116], S. Jaelani[63], C. Jahnke[121], M.J. Jakubowska[142], M.A. Janik[142], M. Jercic[97], O. Jevons[109], R.T. Jimenez Bustamante[105], M. Jin[126], F. Jonas[94,144], P.G. Jones[109], A. Jusko[109], P. Kalinak[65], A. Kalweit[34], J.H. Kang[147], V. Kaplin[91], S. Kar[6], A. Karasu Uysal[77], O. Karavichev[62], T. Karavicheva[62], P. Karczmarczyk[34], E. Karpechev[62], U. Kebschull[74], R. Keidel[46], M. Keil[34], B. Ketzer[42], Z. Khabanova[89], A.M. Khan[6], S. Khan[17], S.A. Khan[141], A. Khanzadeev[96], Y. Kharlov[90], A. Khatun[17], A. Khuntia[118,49], B. Kileng[36], B. Kim[60], B. Kim[133], D. Kim[147], D.J. Kim[127], E.J. Kim[13], H. Kim[147], J.S. Kim[40], J. Kim[102], J. Kim[147], J. Kim[13], M. Kim[102], S. Kim[19], T. Kim[147], T. Kim[147], K. Kindra[98], S. Kirsch[39], I. Kisel[39], S. Kiselev[64], A. Kisiel[142], J.L. Klay[5], C. Klein[69], J. Klein[58], S. Klein[79], C. Klein-Bösing[144], S. Klewin[102], A. Kluge[34], M.L. Knichel[34], A.G. Knospe[126], C. Kobdaj[115], M.K. Köhler[102], T. Kollegger[105], A. Kondratyev[75], N. Kondratyeva[91], E. Kondratyuk[90], P.J. Konopka[34], L. Koska[116], O. Kovalenko[84], V. Kovalenko[112], M. Kowalski[118], I. Králik[65], A. Kravčáková[38], L. Kreis[105], M. Krivda[65,109], F. Krizek[93], K. Krizkova Gajdosova[37], M. Krüger[69], E. Kryshen[96], M. Krzewicki[39], A.M. Kubera[95], V. Kučera[60], C. Kuhn[136], P.G. Kuijer[89], L. Kumar[98], S. Kumar[48], S. Kundu[85], P. Kurashvili[84], A. Kurepin[62], A.B. Kurepin[62], S. Kushpil[93], J. Kvapil[109], M.J. Kweon[60], Y. Kwon[147], S.L. La Pointe[39], P. La Rocca[28], Y.S. Lai[79], R. Langoy[124], K. Lapidus[146,34], A. Lardeux[21], P. Larionov[51], E. Laudi[34], R. Lavicka[37], T. Lazareva[112], R. Lea[25], L. Leardini[102], S. Lee[147], F. Lehas[89], S. Lehner[113], J. Lehrbach[39], R.C. Lemmon[92], I. León Monzón[120], E.D. Lesser[20], M. Lettrich[34], P. Lévai[145], X. Li[12], X.L. Li[6], J. Lien[124], R. Lietava[109], B. Lim[18], S. Lindal[21], V. Lindenstruth[39], S.W. Lindsay[128], C. Lippmann[105], M.A. Lisa[95], V. Litichevskyi[43], A. Liu[79], S. Liu[95], H.M. Ljunggren[80], W.J. Llope[143], I.M. Lofnes[22], V. Loginov[91], C. Loizides[94], P. Loncar[35], X. Lopez[134], E. López Torres[8], P. Luettig[69], J.R. Luhder[144], M. Lunardon[29], G. Luparello[59], M. Lupi[34], A. Maevskaya[62], M. Mager[34], S.M. Mahmood[21], T. Mahmoud[42], A. Maire[136], R.D. Majka[146], M. Malaev[96], Q.W. Malik[21], L. Malinina[75, iii], D. Mal'Kevich[64], P. Malzacher[105], A. Mamonov[107], V. Manko[87], F. Manso[134], V. Manzari[52], Y. Mao[6], M. Marchisone[135], J. Mareš[67], G.V. Margagliotti[25], A. Margotti[53], J. Margutti[63], A. Marín[105], C. Markert[119], M. Marquard[69], N.A. Martin[102], P. Martinengo[34], J.L. Martinez[126], M.I. Martínez[44], G. Martínez

JHEP09(2019)008

García[114], M. Martinez Pedreira[34], S. Masciocchi[105], M. Masera[26], A. Masoni[54], L. Massacrier[61], E. Masson[114], A. Mastroserio[52,138], A.M. Mathis[103,117], P.F.T. Matuoka[121], A. Matyja[118], C. Mayer[118], M. Mazzilli[33], M.A. Mazzoni[57], A.F. Mechler[69], F. Meddi[23], Y. Melikyan[91], A. Menchaca-Rocha[72], E. Meninno[30], M. Meres[14], S. Mhlanga[125], Y. Miake[133], L. Micheletti[26], M.M. Mieskolainen[43], D.L. Mihaylov[103], K. Mikhaylov[64,75], A. Mischke[63, i], A.N. Mishra[70], D. Miśkowiec[105], C.M. Mitu[68], N. Mohammadi[34], A.P. Mohanty[63], B. Mohanty[85], M. Mohisin Khan[17, iv], M. Mondal[141], M.M. Mondal[66], C. Mordasini[103], D.A. Moreira De Godoy[144], L.A.P. Moreno[44], S. Moretto[29], A. Morreale[114], A. Morsch[34], T. Mrnjavac[34], V. Muccifora[51], E. Mudnic[35], D. Mühlheim[144], S. Muhuri[141], J.D. Mulligan[79,146], M.G. Munhoz[121], K. Münning[42], R.H. Munzer[69], H. Murakami[132], S. Murray[73], L. Musa[34], J. Musinsky[65], C.J. Myers[126], J.W. Myrcha[142], B. Naik[48], R. Nair[84], B.K. Nandi[48], R. Nania[10,53], E. Nappi[52], M.U. Naru[15], A.F. Nassirpour[80], H. Natal da Luz[121], C. Nattrass[130], R. Nayak[48], T.K. Nayak[85,141], S. Nazarenko[107], R.A. Negrao De Oliveira[69], L. Nellen[70], S.V. Nesbo[36], G. Neskovic[39], B.S. Nielsen[88], S. Nikolaev[87], S. Nikulin[87], V. Nikulin[96], F. Noferini[10,53], P. Nomokonov[75], G. Nooren[63], J. Norman[78], P. Nowakowski[142], A. Nyanin[87], J. Nystrand[22], M. Ogino[81], A. Ohlson[102], J. Oleniacz[142], A.C. Oliveira Da Silva[121], M.H. Oliver[146], J. Onderwaater[105], C. Oppedisano[58], R. Orava[43], A. Ortiz Velasquez[70], A. Oskarsson[80], J. Otwinowski[118], K. Oyama[81], Y. Pachmayer[102], V. Pacik[88], D. Pagano[140], G. Paić[70], P. Palni[6], J. Pan[143], A.K. Pandey[48], S. Panebianco[137], V. Papikyan[1], P. Pareek[49], J. Park[60], J.E. Parkkila[127], S. Parmar[98], A. Passfeld[144], S.P. Pathak[126], R.N. Patra[141], B. Paul[58], H. Pei[6], T. Peitzmann[63], X. Peng[6], L.G. Pereira[71], H. Pereira Da Costa[137], D. Peresunko[87], G.M. Perez[8], E. Perez Lezama[69], V. Peskov[69], Y. Pestov[4], V. Petráček[37], M. Petrovici[47], R.P. Pezzi[71], S. Piano[59], M. Pikna[14], P. Pillot[114], L.O.D.L. Pimentel[88], O. Pinazza[53,34], L. Pinsky[126], S. Pisano[51], D.B. Piyarathna[126], M. Płoskoń[79], M. Planinic[97], F. Pliquett[69], J. Pluta[142], S. Pochybova[145], M.G. Poghosyan[94], B. Polichtchouk[90], N. Poljak[97], W. Poonsawat[115], A. Pop[47], H. Poppenborg[144], S. Porteboeuf-Houssais[134], V. Pozdniakov[75], S.K. Prasad[3], R. Preghenella[53], F. Prino[58], C.A. Pruneau[143], I. Pshenichnov[62], M. Puccio[26,34], V. Punin[107], K. Puranapanda[141], J. Putschke[143], R.E. Quishpe[126], S. Ragoni[109], S. Raha[3], S. Rajput[99], J. Rak[127], A. Rakotozafindrabe[137], L. Ramello[32], F. Rami[136], R. Raniwala[100], S. Raniwala[100], S.S. Räsänen[43], B.T. Rascanu[69], R. Rath[49], V. Ratza[42], I. Ravasenga[31], K.F. Read[130,94], K. Redlich[84, v], A. Rehman[22], P. Reichelt[69], F. Reidt[34], X. Ren[6], R. Renfordt[69], A. Reshetin[62], J.-P. Revol[10], K. Reygers[102], V. Riabov[96], T. Richert[80,88], M. Richter[21], P. Riedler[34], W. Riegler[34], F. Riggi[28], C. Ristea[68], S.P. Rode[49], M. Rodríguez Cahuantzi[44], K. Røed[21], R. Rogalev[90], E. Rogochaya[75], D. Rohr[34], D. Röhrich[22], P.S. Rokita[142], F. Ronchetti[51], E.D. Rosas[70], K. Roslon[142], P. Rosnet[134], A. Rossi[56,29], A. Rotondi[139], F. Roukoutakis[83], A. Roy[49], P. Roy[108], O.V. Rueda[80], R. Rui[25], B. Rumyantsev[75], A. Rustamov[86], E. Ryabinkin[87], Y. Ryabov[96], A. Rybicki[118], H. Rytkonen[127], S. Saarinen[43], S. Sadhu[141], S. Sadovsky[90], K. Šafařík[37,34], S.K. Saha[141], B. Sahoo[48], P. Sahoo[49], R. Sahoo[49], S. Sahoo[66], P.K. Sahu[66], J. Saini[141], S. Sakai[133], S. Sambyal[99], V. Samsonov[96,91], A. Sandoval[72], A. Sarkar[73], D. Sarkar[141,143], N. Sarkar[141], P. Sarma[41], V.M. Sarti[103], M.H.P. Sas[63], E. Scapparone[53], B. Schaefer[94], J. Schambach[119], H.S. Scheid[69], C. Schiaua[47], R. Schicker[102], A. Schmah[102], C. Schmidt[105], H.R. Schmidt[101], M.O. Schmidt[102], M. Schmidt[101], N.V. Schmidt[94,69], A.R. Schmier[130], J. Schukraft[34,88], Y. Schutz[34,136], K. Schwarz[105], K. Schweda[105], G. Scioli[27], E. Scomparin[58], M. Šefčík[38], J.E. Seger[16], Y. Sekiguchi[132], D. Sekihata[45], I. Selyuzhenkov[105,91], S. Senyukov[136], E. Serradilla[72], P. Sett[48], A. Sevcenco[68], A. Shabanov[62], A. Shabetai[114], R. Shahoyan[34], W. Shaikh[108], A. Shangaraev[90], A. Sharma[98], A. Sharma[99], M. Sharma[99], N. Sharma[98], A.I. Sheikh[141], K. Shigaki[45], M. Shimomura[82], S. Shirinkin[64], Q. Shou[111], Y. Sibiriak[87], S. Siddhanta[54], T. Siemiarczuk[84], D. Silvermyr[80], G. Simatovic[89],

JHEP09(2019)008

G. Simonetti[103,34], R. Singh[85], R. Singh[99], V.K. Singh[141], V. Singhal[141], T. Sinha[108], B. Sitar[14], M. Sitta[32], T.B. Skaali[21], M. Slupecki[127], N. Smirnov[146], R.J.M. Snellings[63], T.W. Snellman[127], J. Sochan[116], C. Soncco[110], J. Song[60,126], A. Songmoolnak[115], F. Soramel[29], S. Sorensen[130], I. Sputowska[118], J. Stachel[102], I. Stan[68], P. Stankus[94], P.J. Steffanic[130], E. Stenlund[80], D. Stocco[114], M.M. Storetvedt[36], P. Strmen[14], A.A.P. Suaide[121], T. Sugitate[45], C. Suire[61], M. Suleymanov[15], M. Suljic[34], R. Sultanov[64], M. Šumbera[93], S. Sumowidagdo[50], K. Suzuki[113], S. Swain[66], A. Szabo[14], I. Szarka[14], U. Tabassam[15], G. Taillepied[134], J. Takahashi[122], G.J. Tambave[22], S. Tang[134,6], M. Tarhini[114], M.G. Tarzila[47], A. Tauro[34], G. Tejeda Muñoz[44], A. Telesca[34], C. Terrevoli[126,29], D. Thakur[49], S. Thakur[141], D. Thomas[119], F. Thoresen[88], R. Tieulent[135], A. Tikhonov[62], A.R. Timmins[126], A. Toia[69], N. Topilskaya[62], M. Toppi[51], F. Torales-Acosta[20], S.R. Torres[120], S. Tripathy[49], T. Tripathy[48], S. Trogolo[26,29], G. Trombetta[33], L. Tropp[38], V. Trubnikov[2], W.H. Trzaska[127], T.P. Trzcinski[142], B.A. Trzeciak[63], T. Tsuji[132], A. Tumkin[107], R. Turrisi[56], T.S. Tveter[21], K. Ullaland[22], E.N. Umaka[126], A. Uras[135], G.L. Usai[24], A. Utrobicic[97], M. Vala[116,38], N. Valle[139], S. Vallero[58], N. van der Kolk[63], L.V.R. van Doremalen[63], M. van Leeuwen[63], P. Vande Vyvre[34], D. Varga[145], M. Varga-Kofarago[145], A. Vargas[44], M. Vargyas[127], R. Varma[48], M. Vasileiou[83], A. Vasiliev[87], O. Vázquez Doce[117,103], V. Vechernin[112], A.M. Veen[63], E. Vercellin[26], S. Vergara Limón[44], L. Vermunt[63], R. Vernet[7], R. Vértesi[145], L. Vickovic[35], J. Viinikainen[127], Z. Vilakazi[131], O. Villalobos Baillie[109], A. Villatoro Tello[44], G. Vino[52], A. Vinogradov[87], T. Virgili[30], V. Vislavicius[88], A. Vodopyanov[75], B. Volkel[34], M.A. Völkl[101], K. Voloshin[64], S.A. Voloshin[143], G. Volpe[33], B. von Haller[34], I. Vorobyev[103,117], D. Voscek[116], J. Vrláková[38], B. Wagner[22], Y. Watanabe[133], M. Weber[113], S.G. Weber[105], A. Wegrzynek[34], D.F. Weiser[102], S.C. Wenzel[34], J.P. Wessels[144], U. Westerhoff[144], A.M. Whitehead[125], E. Widmann[113], J. Wiechula[69], J. Wikne[21], G. Wilk[84], J. Wilkinson[53], G.A. Willems[34], E. Willsher[109], B. Windelband[102], W.E. Witt[130], Y. Wu[129], R. Xu[6], S. Yalcin[77], K. Yamakawa[45], S. Yang[22], S. Yano[137], Z. Yin[6], H. Yokoyama[63], I.-K. Yoo[18], J.H. Yoon[60], S. Yuan[22], A. Yuncu[102], V. Yurchenko[2], V. Zaccolo[58,25], A. Zaman[15], C. Zampolli[34], H.J.C. Zanoli[121], N. Zardoshti[34,109], A. Zarochentsev[112], P. Závada[67], N. Zaviyalov[107], H. Zbroszczyk[142], M. Zhalov[96], X. Zhang[6], Z. Zhang[6,134], C. Zhao[21], V. Zherebchevskii[112], N. Zhigareva[64], D. Zhou[6], Y. Zhou[88], Z. Zhou[22], J. Zhu[6], Y. Zhu[6], A. Zichichi[27,10], M.B. Zimmermann[34], G. Zinovjev[2], N. Zurlo[140]

[i] *Deceased*
[ii] *Dipartimento DET del Politecnico di Torino, Turin, Italy*
[iii] *M.V. Lomonosov Moscow State University, D.V. Skobeltsyn Institute of Nuclear, Physics, Moscow, Russia*
[iv] *Department of Applied Physics, Aligarh Muslim University, Aligarh, India*
[v] *Institute of Theoretical Physics, University of Wroclaw, Poland*

[1] *A.I. Alikhanyan National Science Laboratory (Yerevan Physics Institute) Foundation, Yerevan, Armenia*
[2] *Bogolyubov Institute for Theoretical Physics, National Academy of Sciences of Ukraine, Kiev, Ukraine*
[3] *Bose Institute, Department of Physics and Centre for Astroparticle Physics and Space Science (CAPSS), Kolkata, India*
[4] *Budker Institute for Nuclear Physics, Novosibirsk, Russia*
[5] *California Polytechnic State University, San Luis Obispo, California, U.S.A.*
[6] *Central China Normal University, Wuhan, China*
[7] *Centre de Calcul de l'IN2P3, Villeurbanne, Lyon, France*
[8] *Centro de Aplicaciones Tecnológicas y Desarrollo Nuclear (CEADEN), Havana, Cuba*

JHEP09(2019)008

[9] *Centro de Investigación y de Estudios Avanzados (CINVESTAV), Mexico City and Mérida, Mexico*
[10] *Centro Fermi — Museo Storico della Fisica e Centro Studi e Ricerche "Enrico Fermi', Rome, Italy*
[11] *Chicago State University, Chicago, Illinois, U.S.A.*
[12] *China Institute of Atomic Energy, Beijing, China*
[13] *Chonbuk National University, Jeonju, Republic of Korea*
[14] *Comenius University Bratislava, Faculty of Mathematics, Physics and Informatics, Bratislava, Slovakia*
[15] *COMSATS University Islamabad, Islamabad, Pakistan*
[16] *Creighton University, Omaha, Nebraska, U.S.A.*
[17] *Department of Physics, Aligarh Muslim University, Aligarh, India*
[18] *Department of Physics, Pusan National University, Pusan, Republic of Korea*
[19] *Department of Physics, Sejong University, Seoul, Republic of Korea*
[20] *Department of Physics, University of California, Berkeley, California, U.S.A.*
[21] *Department of Physics, University of Oslo, Oslo, Norway*
[22] *Department of Physics and Technology, University of Bergen, Bergen, Norway*
[23] *Dipartimento di Fisica dell'Università 'La Sapienza' and Sezione INFN, Rome, Italy*
[24] *Dipartimento di Fisica dell'Università and Sezione INFN, Cagliari, Italy*
[25] *Dipartimento di Fisica dell'Università and Sezione INFN, Trieste, Italy*
[26] *Dipartimento di Fisica dell'Università and Sezione INFN, Turin, Italy*
[27] *Dipartimento di Fisica e Astronomia dell'Università and Sezione INFN, Bologna, Italy*
[28] *Dipartimento di Fisica e Astronomia dell'Università and Sezione INFN, Catania, Italy*
[29] *Dipartimento di Fisica e Astronomia dell'Università and Sezione INFN, Padova, Italy*
[30] *Dipartimento di Fisica 'E.R. Caianiello' dell'Università and Gruppo Collegato INFN, Salerno, Italy*
[31] *Dipartimento DISAT del Politecnico and Sezione INFN, Turin, Italy*
[32] *Dipartimento di Scienze e Innovazione Tecnologica dell'Università del Piemonte Orientale and INFN Sezione di Torino, Alessandria, Italy*
[33] *Dipartimento Interateneo di Fisica 'M. Merlin' and Sezione INFN, Bari, Italy*
[34] *European Organization for Nuclear Research (CERN), Geneva, Switzerland*
[35] *Faculty of Electrical Engineering, Mechanical Engineering and Naval Architecture, University of Split, Split, Croatia*
[36] *Faculty of Engineering and Science, Western Norway University of Applied Sciences, Bergen, Norway*
[37] *Faculty of Nuclear Sciences and Physical Engineering, Czech Technical University in Prague, Prague, Czech Republic*
[38] *Faculty of Science, P.J. Šafárik University, Košice, Slovakia*
[39] *Frankfurt Institute for Advanced Studies, Johann Wolfgang Goethe-Universität Frankfurt, Frankfurt, Germany*
[40] *Gangneung-Wonju National University, Gangneung, Republic of Korea*
[41] *Gauhati University, Department of Physics, Guwahati, India*
[42] *Helmholtz-Institut für Strahlen- und Kernphysik, Rheinische Friedrich-Wilhelms-Universität Bonn, Bonn, Germany*
[43] *Helsinki Institute of Physics (HIP), Helsinki, Finland*
[44] *High Energy Physics Group, Universidad Autónoma de Puebla, Puebla, Mexico*
[45] *Hiroshima University, Hiroshima, Japan*
[46] *Hochschule Worms, Zentrum für Technologietransfer und Telekommunikation (ZTT), Worms, Germany*
[47] *Horia Hulubei National Institute of Physics and Nuclear Engineering, Bucharest, Romania*
[48] *Indian Institute of Technology Bombay (IIT), Mumbai, India*
[49] *Indian Institute of Technology Indore, Indore, India*
[50] *Indonesian Institute of Sciences, Jakarta, Indonesia*
[51] *INFN, Laboratori Nazionali di Frascati, Frascati, Italy*
[52] *INFN, Sezione di Bari, Bari, Italy*

JHEP09(2019)008

[53] *INFN, Sezione di Bologna, Bologna, Italy*
[54] *INFN, Sezione di Cagliari, Cagliari, Italy*
[55] *INFN, Sezione di Catania, Catania, Italy*
[56] *INFN, Sezione di Padova, Padova, Italy*
[57] *INFN, Sezione di Roma, Rome, Italy*
[58] *INFN, Sezione di Torino, Turin, Italy*
[59] *INFN, Sezione di Trieste, Trieste, Italy*
[60] *Inha University, Incheon, Republic of Korea*
[61] *Institut de Physique Nucléaire d'Orsay (IPNO), Institut National de Physique Nucléaire et de Physique des Particules (IN2P3/CNRS), Université de Paris-Sud, Université Paris-Saclay, Orsay, France*
[62] *Institute for Nuclear Research, Academy of Sciences, Moscow, Russia*
[63] *Institute for Subatomic Physics, Utrecht University/Nikhef, Utrecht, Netherlands*
[64] *Institute for Theoretical and Experimental Physics, Moscow, Russia*
[65] *Institute of Experimental Physics, Slovak Academy of Sciences, Košice, Slovakia*
[66] *Institute of Physics, Homi Bhabha National Institute, Bhubaneswar, India*
[67] *Institute of Physics of the Czech Academy of Sciences, Prague, Czech Republic*
[68] *Institute of Space Science (ISS), Bucharest, Romania*
[69] *Institut für Kernphysik, Johann Wolfgang Goethe-Universität Frankfurt, Frankfurt, Germany*
[70] *Instituto de Ciencias Nucleares, Universidad Nacional Autónoma de México, Mexico City, Mexico*
[71] *Instituto de Física, Universidade Federal do Rio Grande do Sul (UFRGS), Porto Alegre, Brazil*
[72] *Instituto de Física, Universidad Nacional Autónoma de México, Mexico City, Mexico*
[73] *iThemba LABS, National Research Foundation, Somerset West, South Africa*
[74] *Johann-Wolfgang-Goethe Universität Frankfurt Institut für Informatik, Fachbereich Informatik und Mathematik, Frankfurt, Germany*
[75] *Joint Institute for Nuclear Research (JINR), Dubna, Russia*
[76] *Korea Institute of Science and Technology Information, Daejeon, Republic of Korea*
[77] *KTO Karatay University, Konya, Turkey*
[78] *Laboratoire de Physique Subatomique et de Cosmologie, Université Grenoble-Alpes, CNRS-IN2P3, Grenoble, France*
[79] *Lawrence Berkeley National Laboratory, Berkeley, California, U.S.A.*
[80] *Lund University Department of Physics, Division of Particle Physics, Lund, Sweden*
[81] *Nagasaki Institute of Applied Science, Nagasaki, Japan*
[82] *Nara Women's University (NWU), Nara, Japan*
[83] *National and Kapodistrian University of Athens, School of Science, Department of Physics , Athens, Greece*
[84] *National Centre for Nuclear Research, Warsaw, Poland*
[85] *National Institute of Science Education and Research, Homi Bhabha National Institute, Jatni, India*
[86] *National Nuclear Research Center, Baku, Azerbaijan*
[87] *National Research Centre Kurchatov Institute, Moscow, Russia*
[88] *Niels Bohr Institute, University of Copenhagen, Copenhagen, Denmark*
[89] *Nikhef, National institute for subatomic physics, Amsterdam, Netherlands*
[90] *NRC Kurchatov Institute IHEP, Protvino, Russia*
[91] *NRNU Moscow Engineering Physics Institute, Moscow, Russia*
[92] *Nuclear Physics Group, STFC Daresbury Laboratory, Daresbury, United Kingdom*
[93] *Nuclear Physics Institute of the Czech Academy of Sciences, Řež u Prahy, Czech Republic*
[94] *Oak Ridge National Laboratory, Oak Ridge, Tennessee, U.S.A.*
[95] *Ohio State University, Columbus, Ohio, U.S.A.*
[96] *Petersburg Nuclear Physics Institute, Gatchina, Russia*
[97] *Physics department, Faculty of science, University of Zagreb, Zagreb, Croatia*
[98] *Physics Department, Panjab University, Chandigarh, India*
[99] *Physics Department, University of Jammu, Jammu, India*

JHEP09(2019)008

[100] *Physics Department, University of Rajasthan, Jaipur, India*
[101] *Physikalisches Institut, Eberhard-Karls-Universität Tübingen, Tübingen, Germany*
[102] *Physikalisches Institut, Ruprecht-Karls-Universität Heidelberg, Heidelberg, Germany*
[103] *Physik Department, Technische Universität München, Munich, Germany*
[104] *Politecnico di Bari, Bari, Italy*
[105] *Research Division and ExtreMe Matter Institute EMMI, GSI Helmholtzzentrum für Schwerionenforschung GmbH, Darmstadt, Germany*
[106] *Rudjer Bošković Institute, Zagreb, Croatia*
[107] *Russian Federal Nuclear Center (VNIIEF), Sarov, Russia*
[108] *Saha Institute of Nuclear Physics, Homi Bhabha National Institute, Kolkata, India*
[109] *School of Physics and Astronomy, University of Birmingham, Birmingham, United Kingdom*
[110] *Sección Física, Departamento de Ciencias, Pontificia Universidad Católica del Perú, Lima, Peru*
[111] *Shanghai Institute of Applied Physics, Shanghai, China*
[112] *St. Petersburg State University, St. Petersburg, Russia*
[113] *Stefan Meyer Institut für Subatomare Physik (SMI), Vienna, Austria*
[114] *SUBATECH, IMT Atlantique, Université de Nantes, CNRS-IN2P3, Nantes, France*
[115] *Suranaree University of Technology, Nakhon Ratchasima, Thailand*
[116] *Technical University of Košice, Košice, Slovakia*
[117] *Technische Universität München, Excellence Cluster 'Universe', Munich, Germany*
[118] *The Henryk Niewodniczanski Institute of Nuclear Physics, Polish Academy of Sciences, Cracow, Poland*
[119] *The University of Texas at Austin, Austin, Texas, U.S.A.*
[120] *Universidad Autónoma de Sinaloa, Culiacán, Mexico*
[121] *Universidade de São Paulo (USP), São Paulo, Brazil*
[122] *Universidade Estadual de Campinas (UNICAMP), Campinas, Brazil*
[123] *Universidade Federal do ABC, Santo Andre, Brazil*
[124] *University College of Southeast Norway, Tonsberg, Norway*
[125] *University of Cape Town, Cape Town, South Africa*
[126] *University of Houston, Houston, Texas, U.S.A.*
[127] *University of Jyväskylä, Jyväskylä, Finland*
[128] *University of Liverpool, Liverpool, United Kingdom*
[129] *University of Science and Techonology of China, Hefei, China*
[130] *University of Tennessee, Knoxville, Tennessee, U.S.A.*
[131] *University of the Witwatersrand, Johannesburg, South Africa*
[132] *University of Tokyo, Tokyo, Japan*
[133] *University of Tsukuba, Tsukuba, Japan*
[134] *Université Clermont Auvergne, CNRS/IN2P3, LPC, Clermont-Ferrand, France*
[135] *Université de Lyon, Université Lyon 1, CNRS/IN2P3, IPN-Lyon, Villeurbanne, Lyon, France*
[136] *Université de Strasbourg, CNRS, IPHC UMR 7178, F-67000 Strasbourg, France, Strasbourg, France*
[137] *Université Paris-Saclay Centre d'Etudes de Saclay (CEA), IRFU, Départment de Physique Nucléaire (DPhN), Saclay, France*
[138] *Università degli Studi di Foggia, Foggia, Italy*
[139] *Università degli Studi di Pavia, Pavia, Italy*
[140] *Università di Brescia, Brescia, Italy*
[141] *Variable Energy Cyclotron Centre, Homi Bhabha National Institute, Kolkata, India*
[142] *Warsaw University of Technology, Warsaw, Poland*
[143] *Wayne State University, Detroit, Michigan, U.S.A.*
[144] *Westfälische Wilhelms-Universität Münster, Institut für Kernphysik, Münster, Germany*
[145] *Wigner Research Centre for Physics, Hungarian Academy of Sciences, Budapest, Hungary*
[146] *Yale University, New Haven, Connecticut, U.S.A.*
[147] *Yonsei University, Seoul, Republic of Korea*

JHEP09(2019)008